Autonomous navigation for deep space small satellites
Scientific and technological advances

Turan, Erdem; Speretta, Stefano; Gill, Eberhard

DOI
10.1016/j.actaastro.2021.12.030

Publication date
2022

Document Version
Final published version

Published in
Acta Astronautica

Acta Astronautica 193 (2022) 56–74

Contents lists available at ScienceDirect

Acta Astronautica

journal homepage: www.elsevier.com/locate/actaastro

Autonomous navigation for deep space small satellites: Scientific and technological advances

Erdem Turan *, Stefano Speretta, Eberhard Gill

Delft University of Technology, Faculty of Aerospace Engineering, Kluyverweg 1, 2629 HS, Delft, The Netherlands

ARTICLE INFO

Keywords:
Deep space
Navigation
Communication
Inter-satellite link
Autonomy
Small satellite

ABSTRACT

In recent years, there is a growing interest in small satellites for deep space exploration. The current approach for planetary navigation is based on ground-based radiometric tracking. A new era of low-cost small satellites for space exploration will require autonomous deep space navigation. This will decrease the reliance on ground-based tracking and provide a substantial reduction in operational costs because of crowded communication networks. In addition, it will be an enabler for future missions currently impossible. This review investigates available deep space navigation methods from an autonomy perspective, considering trends in proposed deep space small satellite missions. Autonomous crosslink radiometric navigation, which is one of the best methods for small satellites due to its simplicity and the use of existing technologies, is studied, including available measurement methods, enabling technologies, and applicability to the currently proposed missions. The main objective of this study is to fill the gap in the scientific literature on the autonomous deep space navigation methods, deeply for crosslink radiometric navigation and to aim at showing the potential advantages that this technique could offer to the missions being analyzed. In this study, a total of 64 proposed deep space small satellite missions have been analyzed found from a variety of sources including journal papers, conference proceedings, and mission websites. In those missions, the most popular destinations are found to be cislunar space and small bodies with the purpose of surface mapping and characterization. Even though various autonomous navigation methods have been proposed for those missions, most of them have planned to use the traditional ground-based radiometric tracking for navigation purposes. This study also shows that more than half of the missions can benefit from the crosslink radiometric navigation through the inter-satellite link.

1. Introduction

In previous years, tremendous achievements have been made by deep space small satellites, ranging from asteroid rendezvous and data relay duties. Small satellites usually refer to spacecraft with low mass (<500 kg), including minisatellites (100–500 kg), microsatellites (10–100 kg), nanosatellites (1–10 kg), picosatellites (0.1–1 kg), and femtosatellites (0.01–0.1 kg) [1]. Overall mission success rate and advances in miniaturization enable more small satellite missions to be proposed from universities, companies, and space agencies. The main idea of these mission studies is to enable the exploration of low-cost small satellites for scientific purposes.

Small satellite operations, from ground segment perspective, present several challenges such as tracking multiple spacecraft at the same limited contact time [2], increasing number of missions with limited tracking sources, limited power, and the operational costs of these missions as costs of flight dynamics teams. Due to these challenges, the focus was on autonomous systems. Given the general strive to minimize the overall mission cost, autonomy could be beneficial for such missions. Moreover, navigation systems may benefit the most from autonomy considering the current deep space navigation approach, which is based on traditional ground-based tracking, providing radiometric observables to estimate the position and velocity of the spacecraft. Maneuvering spacecraft is typically performed via commands from ground stations, often impacted by considerable delays.

Autonomous navigation methods are widely investigated in the literature and a few of them have been proposed for deep space missions recently [3–9]. These methods may use existing systems or require additional instruments to estimate the spacecraft's position and velocity. Methods using existing systems have further advantages such as cost and volume reductions.

This study aims to fill the gap in the scientific literature on the autonomous deep space navigation methods considering trends in the small satellites for deep space missions, further investigates one of the most promising autonomous navigation methods, which uses existing systems, called crosslink radiometric navigation. This paper also aims

* Corresponding author.
E-mail addresses: e.turan@tudelft.nl (E. Turan), s.speretta@tudelft.nl (S. Speretta), E.K.A.Gill@tudelft.nl (E. Gill).

https://doi.org/10.1016/j.actaastro.2021.12.030
Received 21 July 2021; Received in revised form 6 November 2021; Accepted 19 December 2021
Available online 6 January 2022

at showing the potential advantages that this technique could offer to the missions being analyzed.

In this study, deep space navigation techniques are categorized based on the measurement method and on the requirement for ground support to highlight recent trends in autonomous navigation. Even though a few methods are proposed for the missions investigated in this study, other possible navigation solutions are also presented in the corresponding sections. Crosslink radiometric navigation uses a inter-satellite communication link, so that it was surveyed whether those missions have capable of inter-satellite communication. Even though this work tried to show existing advances, some missions currently in development, their mission configurations, communication link profiles, and navigation methods might be different from their current status due to lack of information available online at the time of preparing this study. A total of 64 proposed deep space small satellite missions have been analyzed in this study found from a variety of sources including journal papers, conference proceedings, and mission websites. All these missions are provided in Appendix in a structured way, including mission name, size, leading organization, destination, objectives, and corresponding references. Previously, a few deep space CubeSat missions were investigated from a capability point of view in [10]. In [11], architecture trades are studied for an autonomous small spacecraft from a small body exploration. In [12,13], an overview of deep space CubeSat and small satellite developments at JPL is shown. A brief explanation for CubeSats in cislunar space is given in [14]. Communication and ground-based navigation considerations for CubeSats in cislunar space can be found in [15]. However, autonomous navigation for deep space small satellite missions has not been studied so far.

This paper is organized as follows: Section 2 shows the past, present, and future of deep space small satellite missions. In Section 3, deep space navigation methods are explained. In Section 4, the autonomous radiometric navigation method is further investigated, including previous studies in the literature, measurement methods and accuracy, and lastly, enabling technologies. Perspectives for autonomy are given in Section 5. Finally, conclusion is drawn in Section 6.

2. Past, present, and future of deep space small satellite missions

This section introduces past, present, and future of deep space small satellite missions: up to now, various planetary small satellite missions have been successfully performed. Further details of all 64 missions including mission objectives can be found in Appendix.

The first interplanetary micro satellite mission was PROCYON, developed by JAXA and launched together with Hayabusa-2 in 2014 [16]. In 2018, three landers were deployed from Hayabusa-2 to the surface of the asteroid Ryugu and performed their surface mission successfully [17]. Before this, the first spacecraft to land on a comet was Philae by ESA's Rosetta mission in 2014 [18]. Later, Mars Cube One (MarCO), (shown in Fig. 1), was a twin 6U sized first interplanetary CubeSat mission developed by Jet Propulsion Laboratory and launched in May 2018 to accompany the InSight Mars lander [19].

The upcoming launch of Artemis 1, formerly Exploration Mission 1, provides an opportunity for exploring deep space to thirteen 6U sized CubeSats [21](shown in Fig. 2). These CubeSats have a variety of unique mission objectives on the way to the Moon.

NASA's Planetary Science Deep Space SmallSat Studies (PSDS3) program funded 19 studies among received 102 proposals [22]. These concept studies have a variety of destinations such as Mars, Venus, Moon, small bodies, icy bodies, and outer planets [23]. In addition, three proposals, HALO [24], DAVID [24], and MMO [25] have been selected for further technology developments in the SIMPLEx program. The Europa Clipper mission will observe the Europa moon through flybys while orbiting around Jupiter [26]. Three nano-satellites, Mini-MAGGIE [27], DARCSIDE [28], Sylph [29], and Europa Tomography Probe (ETP) [30] are considered as secondary payloads to assist the Europa Clipper mission.

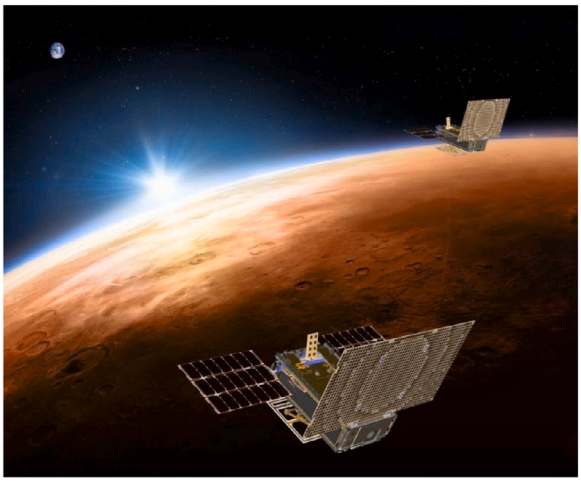

Fig. 1. The first interplanetary CubeSat mission: MarCO [19].

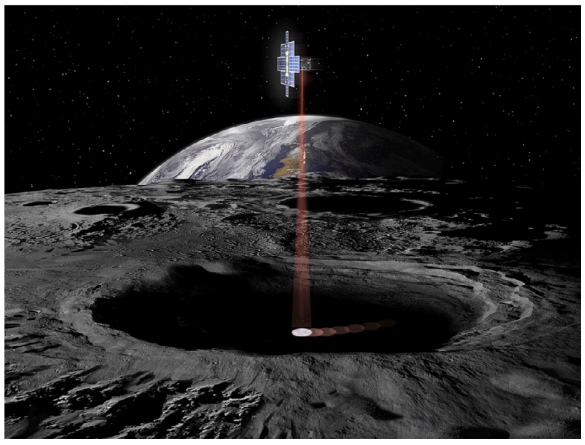

Fig. 2. Lunar Flashlight will use its lasers to search for water on the Moon [20].

Within the third and fourth edition of the Sysnova technical challenges led by the ESA General Studies Programme, a number of studies were performed mainly based on CubeSat Opportunity Payload of Intersatellite Networking Sensors (COPINS) and Lunar CubeSats for Exploration (LUCE) [31]. COPINS objective was to support the ESA Asteroid Impact Mission (AIM). Later on, the mission has changed into the HERA mission. The five CubeSats ASPECT [32], DustCube [33], CUBATA [34], PALS [35] and AGEX [36], mission concepts were selected among several tens of competing concepts for further studies. Thereafter, out of the final selection, only two missions, Juventas and MILANI, have been selected for implementations [37]. In addition, four CubeSats, LUMIO [38], MoonCARE [39], CLE [40] and VMMO [41], concept studies were selected for the LUCE mission among several other concepts. Lastly, a stand-alone deep space CubeSat called M-ARGO (shown in Fig. 3) has been designed to rendezvous with an asteroid and perform close proximity operations [31].

In addition to all mission studies above, there are other concepts such as a radio astronomy enable low frequency space array by aid of recent advances in nano-satellites and investigate the mostly unexplored frequency bands between 0.1–30 MHz [42–45].

Overall, in the near future, small satellites will explore our universe including a variety of destinations as it can be seen in Fig. 4 with various goals summarized in Fig. 5. In general, the trends in destination are in cislunar and small bodies for surface mapping, characterization

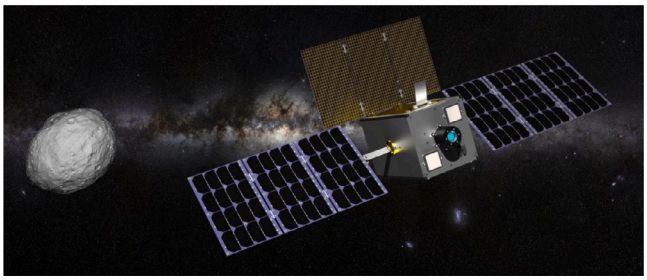

Fig. 3. M-ARGO is a stand-alone deep space CubeSat mission led by ESA [46].

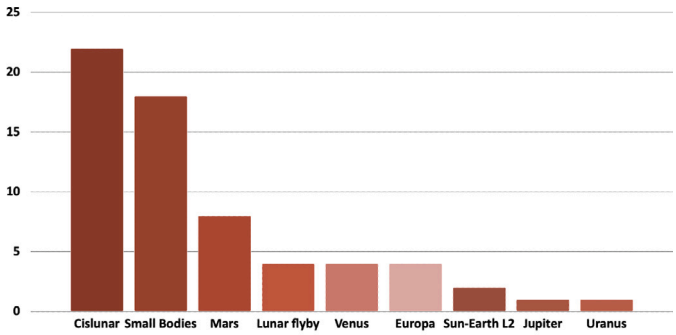

Fig. 4. Deep space small satellite destinations.

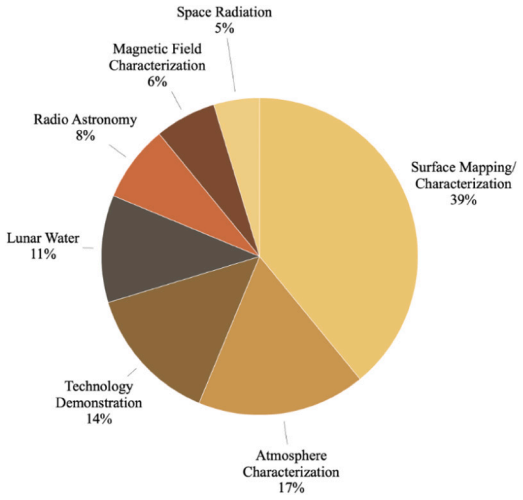

Fig. 5. Key focus areas of deep space missions using small satellites.

purposes. All the mission studies mentioned in this section and analyzed in this survey can be found in Table 1.

3. Deep space navigation methods

Navigation of satellites refers to the mission orbit's knowledge with respect to the central body (absolute) or with respect to another object (relative). It is also related to the knowledge of where the object resides in the past, present (definitive) and future (predictive) [89].

This part of the study shows all reported navigation methods applicable for deep space small satellites. These have been divided into onboard and offboard navigation methods, accounting for the location where navigation knowledge is available (onboard the satellite or on the ground).

Considering current challenges presented by small satellite operations, ground station usage and flight dynamics accounts for a consistent share of the overall mission cost. This is where mission autonomy could help making the mission fit tighter cost caps. Fully autonomous navigation is only possible if it can be performed on-board without any intervention from the ground [5]. If the on-board observations are collected by the aid of ground-based link and/or processed on ground assets, this approach would be named as semi-autonomous navigation. In other words, semi-autonomous methods may use one-way measurements collected by spacecraft where the navigation is performed and/or received processed data by ground assets. Basically, autonomous navigation is only possible if the data is collected and processed on-board. On the other hand, non-autonomous navigation methods are based on ground station observations, and/or ground data processing. This is why they have been named as off-board in this study.

In general, autonomy could be advantageous to reduce mission cost or increase performances [8]. Autonomy can provide minimal-cost if ground operations or hardware are reduced and lead to increased performance if the spacecraft performs a specific task faster or better than a ground-based system. In addition, there might be tasks which cannot be done without autonomy. In the past, autonomous navigation has been used on a few deep space missions such as Deep Space 1 (DS1) [3,4,90], STARDUST [91], Deep Impact (DI) [92] which are all supported by JPL's Autonomous Optical System (AutoNAV) [90,93], and SMART-1 [94]. In those missions, the preferred approach was to compute their position and trajectory correction maneuvers using ground station observations [95,96]. This approach was also true for small spacecraft like Philae-Rosetta, HAYABUSA-1 [97], and MarCO CubeSats [95].

Fig. 6 presents an concept breakdown diagram showing different navigation approaches for deep space. The following sub-sections present a summary of these options referring to small satellite missions that planned to use the relevant method. A few options are not considered for the missions investigated in this study so that these methods are collected under the same title as other methods. These options are summarized in with an illustration given in Fig. 7.

3.1. On-board data collection

This subsection will clarify navigation methods which collect observables on-board without any intervention from ground assets. In the next parts, various fully and semi-autonomous navigation options will be summarized.

3.1.1. Optical navigation

Optical navigation refers to a variety of methods of determining the spacecraft states, relative position and velocity, between a spacecraft and a target body or bodies with on-board optical sensors. Basically, optical sensors, in which their characteristics determine resolutions, sensitivities, and uncertainties, estimate Line-of-Sight (LOS) to beacons or to known locations at the surface [98]. In principle, optical navigation methods compute a body position in the camera reference frame and derive target location in space from its location in the images [98]. These methods in general can be categorized based on the apparent size of the target body on the observed image. The key categories dividing methods from each other are unresolved and resolved center finding, limb based and surface landmark based navigation [89]. The main advantage of these methods is that can be used in various mission phases such as cruise, flyby, rendezvous, orbiting and landing. The data used for vision-based navigation consist of digital pictures which contain various kind of noise sources such as shot noise, read noise, dark current, fixed pattern noise, and quantization noise [99]. Few deep space missions, such as, for example, Deep Space 1, STARDUST, Deep Impact, and EPOXI used the JPL's Autonomous Optical System (AutoNAV) [90,93] implementing such methods. For the DS1 mission,

Table 1
Analyzed mission IDs and references.

Cislunar Missions		Small Bodies		Others	
Lunar Flash Light	[21]	Juventas	[37,47]	MarsDROP	[48]
Lunar Ice Cube	[49]	MILANI	[37,50]	MAT	[23,51]
LunaH-Map	[52]	ASPECT	[32]	MARIO	[53]
LunIR	[54]	Dust Cube	[33]	MarCO	[55]
ArgoMoon	[56]	PALS	[35]	MMO	[57]
OMOTENASHI	[58]	CUBATA	[34]	Aeolus	[23,59]
Cislunar Explorers	[14,60]	AGEX	[36]	MISEN	[23,61]
EQUULEUS	[62]	B1	[63,64]	MIIAR	[65]
HALO	[24]	B2	[63,64]	Cupid's Arrow	[23,66]
WATER	[23,67]	BIRDY-T	[7]	SNAP	[23,68]
IMPEL	[23,69]	AI3	[70]	CUVE	[23,71]
CubeX	[23,72]	NEA Scout	[21]	ETP	[29,30]
LUMIO	[31,38]	M-Argo	[31]	Mini-Maggie	[27]
VMMO	[31,41]	DAVID	[25]	DARCSIDE	[28]
CLE	[31,40]	Ross	[23,73]	Sylph	[29]
MoonCare	[31,39]	APEX	[23,74]	SAEVe	[23,75]
NanoSWARM	[76]	PRISM	[23,77]	DEx	[44]
MiLuV	[23,78]	PrOVE	[23,79]	SULFRO	[45]
BOLAS	[23,80]			JUMPER	[23,81]
OLFAR	[42]			VAMOS	[23,82]
DSL	[43]				
CAPSTONE	[83]				
CuSP	[84]				
BioSentinel	[85]				
CU-E3	[86]				
Team Miles	[87,88]				

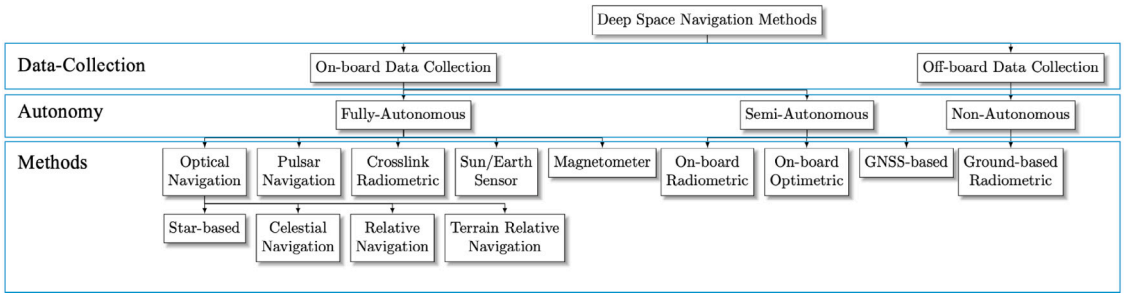

Fig. 6. Deep space navigation methods.

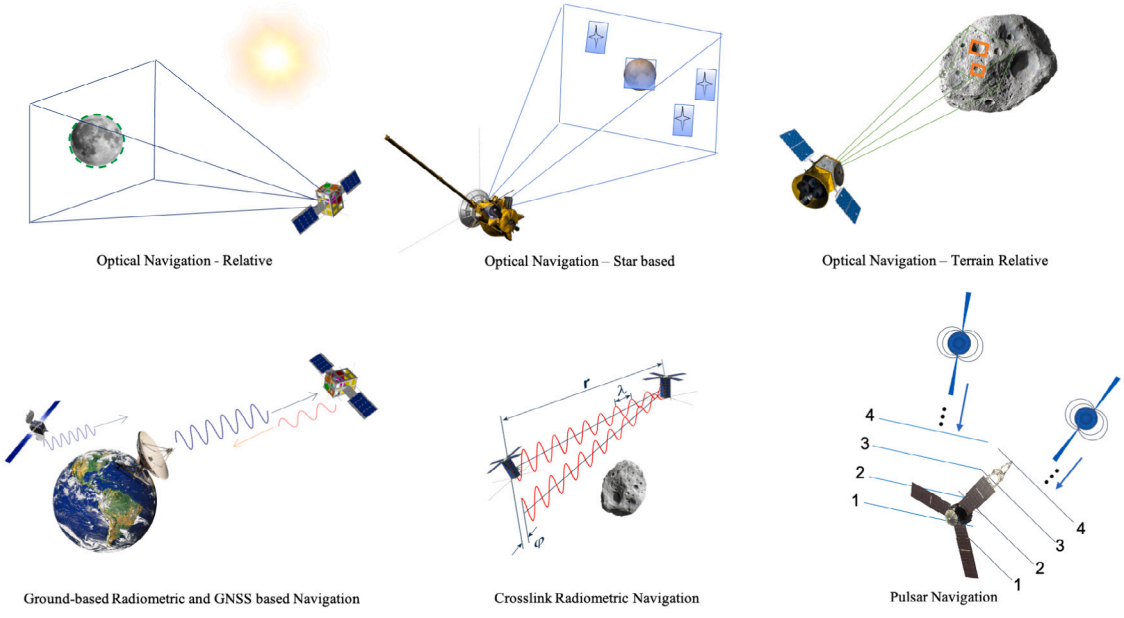

Fig. 7. Illustration of deep space navigation methods.

less than 150 km position and 0.2 m/s velocity accuracies have been achieved during the cruise phase [93].

Regarding optical navigation methods, Star based and Celestial Navigation methods use inertial pointing and bearing observations respectively. Relative Navigation generates bearing and/or position estimates to an observed object [100]. Lastly, Terrain Relative Navigation combines together on-board optical data with a map of the landing area to avoid landing hazards.

A few deep space small satellite missions have planned to use one of the proposed optical methods. In the In-Flight Orbit Determination (IFOD) system part of the BIRDY-T mission combines optical measurements of foreground objects, an asynchronous triangulation and a Kalman filter to determine the trajectory on the way of Mars in the cruise phase [101]. In the LUMIO mission, the Moon full disk size of an image is linked with the real one to estimate the position and velocity of spacecraft in a halo orbit at the Earth–Moon L2 [6]. By studying the sizes of the Earth, the Moon and the Sun and their locations relative to each another, the Cislunar Explorers mission, for example, will estimate their positions within tens of kilometers in cislunar space [102,103]. In the M-ARGO mission, miniaturized on-board optical sensors will provide line-of-sight measurements to fed the navigation filter [104]. In the good observation conditions, navigation accuracy is expected in the order of 1000 km (3σ) for the position and 1 m/s (3σ) for the velocity components [104].

In brief, optical navigation provides major advantages over other architectures, such as moderate to high accuracy navigation solutions, while being compatible with all mission phases.

3.1.2. Pulsar navigation

X-ray pulsar navigation uses the periodic X-ray signals emitted from pulsars to estimate the spacecraft states, by estimating the time- and direction-of-arrival of the pulses with a single instrument. Stable neutron stars spinning nearly 1000 times a second, for example, can provide a solution for autonomous navigation: the pulse Time-of-arrival data for each pulsar is collected and compared with an ephemeris database and after that Time-of-arrival data is used to determine or to update attitude, position, velocity of a spacecraft [105]. The most significant benefit of this method is providing an opportunity to stabilize on-board clocks via the periodic pulse arrivals [105]. Furthermore, this method can be used for missions not only in close proximity to the Earth but also in deep space. The Station Explorer for X-ray Timing and Navigation Technology (SEXTANT) mission showed that 10 km RSS position error could be achievable with this method for the International Space Station [9,106].

Pulsar navigation methods determining the position of spacecraft are similar to optical celestial navigation [105]: however, pulsars are easier to detect. One of them, Pulsar elevation method uses elevation angles between the signal source and receiver, and apparent diameter of the body, to determine the distance which provides position determination with the help of multiple X-ray sources. Another method is limb occultation which uses the time spend behind a planetary body to determine a chord length of the body. When the body dimensions and the source position are known, the position can be determined [105]. There are several error sources in timing measurements made from X-ray pulsars such as Poisson fluctuations, phase detector offset, position-timing, pulse frequency knowledge, local oscillator fluctuations, random fluctuations [107].

CubeX will demonstrate the feasibility of this concept as a CubeSat with two X-ray instruments, an X-ray Imaging Spectrometer and a Solar X-ray Monitor, using X-ray millisecond pulsars at the Lunar orbit [72]. On the other hand, radio frequencies that pulsars emit are from 100 MHz to a few GHz. In order to detect those signals, radio frequency systems would require very large antennas [108] (>25 m in diameter) which is not feasible for small satellites.

Overall, pulsar navigation provides more accurate navigation solution over optical navigation (less than 0.1 km position accuracy at 1AU with 10^{-7} s timing and 10^{-4} arcsec pulsar position errors [105]). One important advantage is the possibility of stabilizing the on-board clocks via the periodic pulsar signals while a major disadvantage is the sensor size and the required integration time, preventing operations in some mission phases, such as close-proximity.

3.1.3. Crosslink radiometric navigation

Inter-satellite radiometric observables such as range and range-rate provide a relative navigation solution for distributed satellites systems with more than one spacecraft. This method is very useful for small satellites, especially for those being carried by another spacecraft (mothercraft): due to limited on-board power for communication and data transmission, deep space small satellite missions would use a one-hop link configuration to transmit all the scientific data to ground. Existing inter-satellite communication links can also be used for navigation aspects.

In order to estimate the absolute position and velocity of a spacecraft without using any ground-based observation (for the purpose of autonomous navigation), the size, shape, and orientation of the spacecraft orbit must be observable from the available radiometric measurements between satellites [109,110]. The observability of the system, thus, depends on one of the satellites occupying an unique trajectory [109] to be used as an absolute reference. From the scientific perspective, the observability of the system can be tested either via calculating the rank of the observability matrix or via the condition number cond(λ) with the following information matrix λ over the time period $[0, T]$:

$$\lambda = \int_0^T \Phi^T(t)\tilde{H}^T(t)W(t)\tilde{H}(t)\Phi(t)dt \tag{1}$$

where $\tilde{H}(t)$ the linearized matrix that maps states into measurements, $\Phi(t)$ the state transition matrix, $W(t)$ the weighting matrix. If the matrix has a full rank, meaning all the rows are not dependent, the system is observable and the navigation filter can estimate all states [111]. However, the $\tilde{H}(t)$ matrix, which is the partials of measurements with respect to estimated states, would make the rows of λ dependent, because many of them are equal in magnitude and opposite in sign [8]. This is mainly due to relative position vector between satellites. But, the differences between the state transition matrices $\Phi(t)$ of the satellites make system observable, and λ positive definite [8]. Therefore, absolute positions of a spacecraft could be estimated via crosslink measurements in the three-body problem but it could not be estimated in the two-body problem. This is linked with the asymmetry of the gravity field allowing unique orbital configurations to exist [109]. In other words, the acceleration function acting on a spacecraft determines whether there is an unique orbit or not and thus absolute state estimation is possible or not. In a symmetrical acceleration field, in the two-body problem for instance, there is no unique orbit because the acceleration function and its time derivative are symmetric [109]. This is why in the two-body problem, the absolute orientation of the orbital plane could not be observed via crosslink measurements but only the relative orientation [8,111]. The Linked, Autonomous, Interplanetary Satellite Orbit Navigation (LiAISON) method [110] is based on inter-satellite radiometric measurements to estimate spacecraft absolute states when at least one of the orbits has a unique size, shape, and orientation. This can be found in several deep space cases such as around asteroids or at libration points. For example, third-body perturbations of the Moon are sufficient for unique orbits at Earth–Moon libration points to exist. This navigation architecture will be tested in the CAPSTONE mission based on the communication link between Lunar Reconnaissance Orbiter (LRO) and CAPSTONE CubeSat (shown in Fig. 8) at the Lunar vicinity [83].

In short, this method has an advantage over other navigation methods if the mission consists of multiple spacecraft, especially when one of the spacecraft has a trajectory in a highly asymmetrical gravity field.

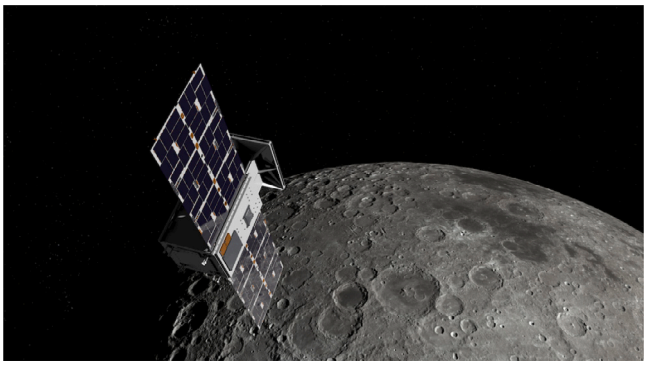

Fig. 8. CAPSTONE will be the first cislunar CubeSat and will perform spacecraft-to-spacecraft radiometric navigation [83].

The most important advantage of this method is the use of existing communication systems without require any additional instruments. This method though cannot be used in a standalone missions and it does not provide any attitude solution (see Figs. 8, 9 and 13).

3.1.4. Others

This part of the study focuses on alternative methods based on specific features which make them best for a very specific mission category. Autonomous orbit determination was first proposed and analyzed by Markley [112,113] for an Earth-orbiting spacecraft with a method based on Sun/Earth sensors. The Sun Doppler method, for example, is based on sun-light Doppler shift measurements with a spectrometer combining directional data measurements collected from Earth and Sun sensors provides an autonomous navigation solution within an accuracy of 3 km in position for an interplanetary spacecraft [114]. A magnetometer is another option that provides a measurement of the local magnetic field to estimate the attitude and orbital position of a spacecraft. This approach could be used on a destination where the magnetic field has been sufficiently characterized [9].

Semi-autonomous methods, like on-board radiometric and optimetrics, use almost the same approach which is based on one-way forward radio or laser signal to spacecraft from ground stations. Meter-level accuracy could be achieved for a spacecraft at the Moon with an on-board optimetric method [100]. GNSS-based navigation is a feasible solution for missions where a global positioning system has been deployed. This is currently applicable for orbits around Earth and in the cislunar environment [115].

3.2. Off-board data collection

Ground-based radiometric navigation is the traditional method used to estimate the spacecraft states in deep space. Most of the missions, such as Lunar IceCube, LunaH-Map, EQUULEUS, and others in this study plan to use traditional ground-based tracking for navigation purposes, thanks to the relative geometry between Earth and the deep space final destination for the full mission duration. In case ground-based tracking is a baseline for navigation strategy, tracking frequency becomes an important parameter to meet the mission requirements. Weekly tracking, in general, would be sufficient to meet navigation requirements for a deep space mission. When special navigation error requirements are present (such as 100 m in position and 0.1 cm/s velocity) tracking would be required every 2–3 days for cislunar missions as it planned for Lunar IceCube [15]. Regarding ranging error, sub-1 m level can be considered as achievable accuracy requiring long correlation and integration times. Many small satellites would not need the high accuracy for the ranging measurement [116].

4. Autonomous radiometric navigation

This section investigates autonomous radiometric navigation methods used by the missions presented in Section 2 and Appendix. The communications trend in deep space small satellite missions proposed up to now shows the common interest in inter-satellite link (ISL): almost 58% of the analyzed missions have planned to use inter-satellite link for telemetry, telecommand or tracking purposes. The reason behind this trend, in general, is the limited power available for communication on small satellite. Those missions can be categorized based on their link profile and destinations, as it can be seen in Table 3. Considering the present and future relevance of distributed space system missions and the trend towards cost reduction and performance improvement, autonomous navigation can be seen as a promising technique. Inter-satellite radiometric measurements can be thus used to achieve relative navigation but also, depending on the specific mission characteristics, to achieve absolute navigation solutions.

4.1. Crosslink radiometric navigation

Up to now, there have been many studies on inter-satellite measurement based autonomous navigation of Earth orbiting satellites. The estimation accuracy for this case depends on the relative spacecraft position and velocity. Furthermore, navigation uncertainty increases as orbits are close to each other [117]. It is shown in [118] that including J2 perturbation into the models makes the system more observable. Moreover, there have been studies on combining relative range and angle measurements [118,119]. Inter-satellite range measurements are more critical than relative angle measurements as long as the observability issue is solved [119] . However, relative range measurements only are not sufficient to determine the full states, position and velocity, in Earth orbiting satellites (This is also called the rank defect problem [119]). Even adding relative velocity measurement in addition to relative ranging does not provide a full state estimation [120]. This is also true in case the spacecraft is orbiting very close to the primary body. Still, this can be enough to meet navigation requirements for certain missions, such as an asteroid flyby, due to the short duration.

The Linked, Autonomous, Interplanetary Satellite Orbit Navigation (LiAISON) is proposed in [110]. This is an orbit determination method which uses satellite-to-satellite observations, such as range and/or range-rate, to estimate absolute states of spacecraft. Such an architecture can be used when at least one of orbits has a unique size, shape, and orientation as it can be found in several deep space cases such as around asteroids or libration point orbits. The characteristics of the acceleration function is the main factor to decide whether inter-satellite range or range-rate measurements can be used alone to estimate the absolute states of spacecraft. In the symmetrical acceleration field, for example, there is no unique orbits because the acceleration function and its time derivative are symmetric. It was also mentioned in [109], uncertainties in the force model and observation noise can prevent satellite-to-satellite tracking orbit determination. In other words, acceleration functions with sufficient asymmetry are needed to overcome uncertainties in models and noise in observations. Improving the performances of the LiAISON architecture requires increasing inter-satellite distances. The more satellites increase the overall navigation accuracy. On the other hand, multiple satellites on the same orbital plane decrease the achievable accuracy due to observability issues. [111] provides an analysis for various possible geometrical configurations for coplanar and non-coplanar situations in two-body problem showing non-coplanar configurations provide better navigation results.

This architecture has been applied to missions at asteroids, libration points, and cislunar vicinity and a summary of the mission concepts studies can be seen in Table 4. In those mission scenarios, the effect of different observations is also investigated. In one of those, LiAISON supplemented by an optical navigation system achieved

Table 2
Deep space navigation methods overview.

Navigation Methods	Advantages	Disadvantages	Examples	References
Optical Navigation	Compatible with all mission phases Moderate to high accuracy	Moderate to high cost	BIRDY-T, LUMIO, Sylph, NEA-Scout, Juventas, IMPEL, DustCube, Cubata, PALS, M-ARGO	[6,101,104]
Pulsar Navigation	High accuracy	Sensor size Unavailable for rendezvous	CubeX, OLFAR	[72]
Crosslink Radiometric	High accuracy Uses existing systems	Requires multiple spacecraft	CAPSTONE	[83]
Sun/Earth Sensor	Mature sensor Compatible with other systems	Limited availability	–	[114]
Magnetometer	Mature sensor Compatible with other systems	Available only in characterized magnetic fields	–	[9]
GNSS-based	High accuracy	Available only in cislunar vicinity Sensor size	–	[115]
One-way Forward Link	High accuracy with optimetrics	Not autonomous	–	
Ground-based Radiometric	Heritage	Not autonomous	Lunar IceCube, LunaH-Map, EQUULEUS, JUMPER, OMOTENASHI, CuSP, Lunar Flashlight, Biosentinel	[15,116]

Table 3
Categorization of 64 satellites based on their communication links and destinations, red indicates > 2 number of satellites, blue = 2 satellites, black a single satellite. Missions indicated as black in the inter-satellite link column have crosslink with the mothercraft/carrier spacecraft.

	Inter-Satellite Link (ISL) Only	Direct-to-Earth Link (DTE) Only	ISL & DTE Link	Total Number
Cislunar	LUMIO, VMMO, CLE, MoonCare, NanoSWARM	Lunar Flash Light, Lunar Ice Cube, LunaH-Map, LunIR, ArgoMoon, OMOTENASHI, Cislunar Explorers, EQUULEUS, HALO, WATER, IMPEL, CubeX	MiLuV, BOLAS, OLFAR, DSL CAPSTONE	22
Mars	MarsDROP	MAT, MARIO	MarCO, MMO, Aeolus, MISEN, MIIAR	8
Small Bodies	Juventas, MILANI, ASPECT, Dust Cube, PALS, CUBATA, AGEX, B1, B2, BIRDY-T, AI3	NEA Scout, M-Argo, DAVID,Ross PrOVE	APEX, PRISM	18
Venus	Cupid's Arrow, SAEVe	CUVE, VAMOS		4
Jupiter		JUMPER		1
Uranus	SNAP			1
Europa	ETP, Mini-Maggie, DARCSIDE, Sylph			4
Sun-Earth L2			DEx, SULFRO	2
Lunar flyby trajectory		CuSP, BioSentinel, CU-E^3, Team Miles		4
Total Number	24	26	14	64

sub-meter level estimation accuracy for missions around asteroid 433 Eros [121]. Adding ground-based radiometric measurements would further increase the navigation accuracy at the expense of partial autonomy [122]. In addition to the effect of observations, modeling errors and filtering methods have also been studied so far. The high fidelity measurement models are used for distance retrogate orbiter in cislunar space to see the effect of satellite-borne clock errors [123]. Lastly, novel filtering methods are also studied for the LiAISON architecture in [124].

Comprehensive studies have demonstrated the LiAISON algorithm's capabilities over the past decade [8,110,121–123,125–128]. The general trend is that LiAISON provides excellent results for cases around asteroids and lunar-Lagrangian points and less accurate results for cases in which orbiters are very close to each other and the gravitational body, such as lunar orbiters.

Overall, the crosslink radiometric navigation accuracy and feasibility depends on various parameters: measurement type, accuracy, interval, inter-satellite distance, number of spacecraft, orbital size, shape and orientation. Measurement types are mainly range and range rate observables with typical 1-sigma accuracy (DTE link) of 2 m and 0.1 mm/s respectively [129]. Increasing the measurement interval and the number of spacecraft in the architecture has a positive impact on navigation accuracy. On the other hand, decreasing inter-satellite distance reduces navigation accuracy. Lastly, non-coplanar orbits provide better solutions than coplanar orbits due to better observability.

The LiAISON concept mainly takes its strength from the asymmetry in the gravity field, their unique orbits, and inter-satellite distances; Table 5 shows the applicability for radiometric autonomous navigation for small satellites with an inter-satellite link. Spacecraft around small bodies experience the asymmetrical gravity field the most. This makes them highly applicable for autonomous radiometric navigation. On the other hand, spacecraft flying very close to primary bodies, such as Mars, experience less asymmetric perturbations. This means those missions cannot be fully applicable for this type of concept. This shows that almost 81% of the missions capable of inter-satellite link could benefit by using radiometric autonomous navigation by using only existing communication systems.

4.2. Radiometric measurement techniques

Radiometric measurements, in general, rely on range and range-rate measurements. Ranging methods [130] are in general divided

Table 4
Summary of relevant selected LiAISON studies in the literature.

Author	Mission Orbit	Number of S/C	Ground Obs.	Inter-satellite Measurement	Estimation Technique	Position Accuracy	Velocity Accuracy
Hill (2008)	Earth–Moon L2 Halo-Low Lunar Orbiter	2	No	Range (RF)	EKF	Halo S/C 78.68 m (RSS) Lunar Orbiter 2.93 m (RSS)	Halo S/C 5.3×10^{-4} m/s (RSS) Lunar Orbiter 2.59×10^{-3} m/s (RSS)
Hill (2008)	Lunar Frozen Constellation	3	No	Range (RF)	EKF	Sat1- 1905.68 m (RSS) Sat2 and Sat3 N/A	N/A
Hill (2008)	Hybrid EM L2 Frozen Orbit Constellation	2	No	Range (RF)	EKF	Halo S/C 87 m (RSS) Frozen Orbiter 9.8 m (RSS)	Halo S/C 0.4×10^{-3} m/s (RSS) Frozen Orbiter 1.4×10^{-3} m/s (RSS)
Hill (2008)	Earth–Moon L1 LEO Constellation	2	No	Range (RF)	EKF	Halo S/C 512 m (RSS) LEO S/C 11 m (RSS)	N/A
Leonard (2012)	Asteroid(433 Eros)	2	Both	Range, Doppler (RF)	EKF	Sat1 55.92 m (RMS) Sat2 37.46 m (RMS) Around 10 m with DSN	Sat1 5.6×10^{-3} m/s (RMS) Sat2 3.5×10^{-3} m/s (RMS)
Hesar (2012)	Asteroid(433 Eros)	2	Yes	Range, Doppler (RF)	EKF	Sub-meter level	N/A
Hesar (2015)	Earth–Moon L2 Halo-Surface Asset	2	Both	Range, Doppler (RF)	EKF	Order of 10 m	N/A
Fujimoto (2016)	Asteroid(433 Eros)	11	No	Range, Angles, Angle Rate (Visual)	EKF	Order of 1 m	$\sim 10 \times 10^{-4}$ m/s
Stacey (2018)	Asteroid(433 Eros)	3	No	Range, Doppler, Angles, Angle Rate (RF+Visual)	UKF	Order of 1 m	$\sim 10 \times 10^{-6}$ m/s
Wang (2019)	DRO in cislunar space Lunar Orbitter	2	No	Range (RF)	EKF	Order of 100 m	$\sim 10 \times 10^{-4}$ m/s
Tong (2019)	Observability analysis in two-body dynamics	2	No	Range (RF)	UKF	Order of 100 m	$\sim 10 \times 10^{-1}$ m/s

Table 5
Categorization of small satellite missions having inter-satellite links based on applicability of LiAISON autonomous navigation architecture, red indicates > 2 number of satellites, blue = 2 satellites, black a single satellite (ISL with mothercraft).

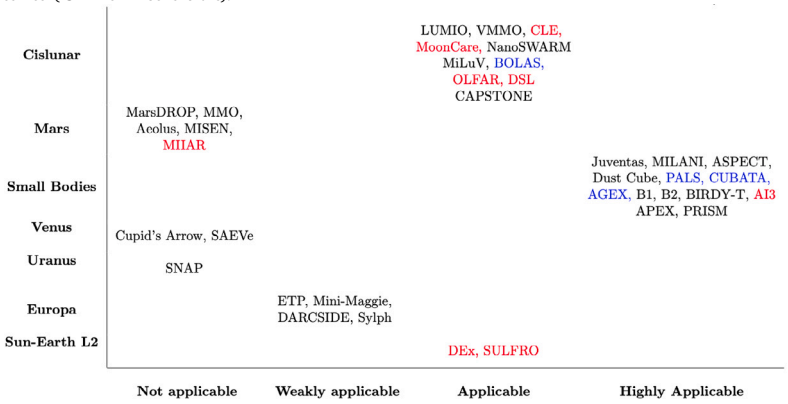

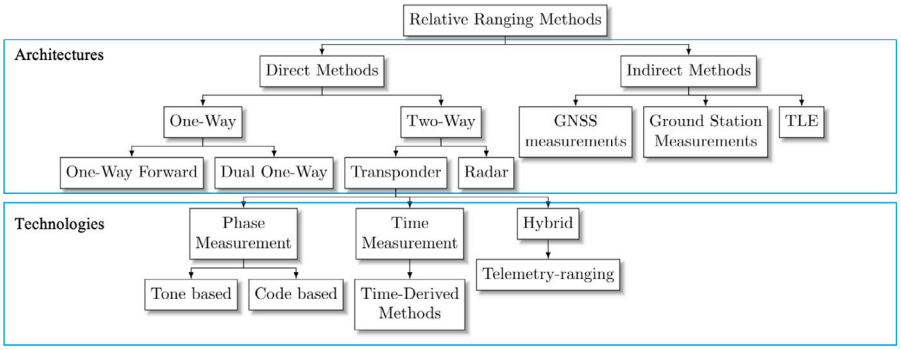

Fig. 9. Relative ranging methods.

into direct and indirect ones, depending on how the inter-satellite distance is measured. Indirect methods may derive the distance from other measurements such as (in the case of Earth-bound systems) GNSS measurements, TDRS, PRARE, DORIS [130]. The inter-satellite ranging (shown in Fig. 9) methods can be divided into two subgroups as indirect and direct methods. Indirect ranging methods include the subtraction of two ranging measurements for which the difference yields the inter-satellite distance. For Earth-orbiting satellites, this can be done using GNSS measurements, tracking data via the ground station, TDRS system, PRARE, or two-line elements provided by NORAD [130]. For the Deep Space missions, indirect inter-satellite ranging can only be done by using ground stations.

Direct inter-satellite distance can be acquired via inter-satellite ranging measurements. This can be useful when indirect measurements are not available, or autonomy is desired. Direct measurements can also be split into two subcategories, as one-way or two-way. Time synchronization between spacecraft is the main problem for the one-way ranging methods: If the clocks are perfectly synchronized, accurate one-way ranging is possible but this is very hard to achieve in practice. Two-way ranging can be performed in two ways: transponder-based and radar-based. The main difference between these two methods is that radar measurements use the signal reflected by the target (the return signal power scales with the fourth power of the distance) while transponders regenerate and re-transmit the return signal (with the return signal power scaling only with the second power of distance). Transponders require transmission and reception to happen almost at the same time, forcing the system to operate on two separate frequencies. This greatly reduce the required transmission power and allows to estimate and compensate frequency-dependent phenomenons, like plasma effects. Distance is then calculated by measuring the round-trip light time: propagation through active components (such as the electronic systems in the transponder) or through passive systems (like antennas and cabling) can introduce a propagation delay up to few micro seconds [131] that can be statically compensated for. One effect to also account for with transponders is the repetitive nature of the ranging signal used, leading to a distance ambiguity (the ESA ranging system has, for example, a range ambiguity of 18000 km [132]) that can be easily compensated for with a-priori pre-measurements or fitting the spacecraft states with orbital models.

4.2.1. *Phase measurements*

Phase measurements are a very common technique to estimate distance by comparing the phase shift between the transmitted and received ranging signal, converting then the phase offset into a distance. This still requires the phase ambiguity to be solved in case the ranging signal period exceeds the roundtrip light time. Common standards used for this purpose are: signal replication based tone standards (Sequential tone [133], ESA-tone [134], ESA-like, USB tone [135]), direct phase measurement based standards (INMARSAT tone, LMCO tone [135]) and pseudoranging standards (JPL PN code, CCSDS T4B and T2B codes [136,137]) and lastly, combination of tone and code, ESA code standard [132]. It should be noted that such standards are used for ranging measurements between a ground station and an orbiting satellite and often require an operator to control the ranging process, limiting the achievable autonomy. Due to these standards and long correlation time, measurements with a standard deviation of one meter have been made for an interplanetary spacecraft, even with small signal-to-noise ratios [138]. Similar standards cannot be used for inter-satellite ranging due to the complexity of the system: satellite modems often have a lower set of functionalities, which often drove the developments of separate standards [139] using similar techniques but adapted to the inter-satellite case.

There are various challenges with small satellites in terms of tracking, and there are the limitations of the small satellites themselves. Due to power limitations on small satellite, communication window is typically limited and this is often more severe for direct-to-Earth links due to the higher transmit power required, with respect to inter-satellite links. Furthermore, there can be a limitation for transponders regarding the data rate that can be generated. One of the earlier studies [116] mentioned that there is a limitation on the achievable data rate, which is affected by the ranging signal. The turn around ranging signal, which is modulated by the spacecraft's transponder, reduces the power available for telemetry if the ranging signal is used for its orbit determination. In other words, the ranging signal affects the supported data rate adversely. Having separate tracking and telemetry sessions may overcome this problem but the limited contact time should be considered for such cases.

4.2.2. Time measurements

Another way to compute the inter-satellite distance is based on time transfer: time correction, correlation and distribution are services provided by the Consultative Committee for Space Data Systems (CCSDS) Proximity-1 Space Link Protocol [140]. Users can use these services to exchange times between satellites and derive time-derived ranging measurements using dedicated algorithms to deal with physical limitations (such as the on-board clock stability). Efficient and reliable time exchange and processing algorithms are proposed in [141,142] for the use of space data link between spacecraft in the vicinity of Mars and Moon. Basically, time-derived ranging is very useful for ISL based applications and the process is shown in more details in Fig. 10; t_1 is the S/C A timestamp at the time of transmission to S/C B, while t_2 is the reception timestamp on S/C B. Similarly, t_3 and t_4 are the S/C A and S/C B timestamps at the time of transmission and reception respectively. When each S/C obtains the four successive timestamps, the round trip light time and offset can be calculated [141]. It should be remembered that the time tags are latched from the spacecraft clock, whose rate could drift from the liftoff nominal value. Further processing of the time tags requires the conversion to a coordinated-time timestamp for easier correlation and comparison with other spacecraft.

A very similar method was proposed in [143], where the round-trip light time was measured from ping requests directly using the satellite radio (removing all un-needed processing steps to guarantee repeatable measurements). From the hardware testing, a ranging accuracy was found to be a 1σ error of $0.156\,\mathrm{km}$ under strong signal conditions and $0.303\,\mathrm{km}$ under realistic worst-case conditions for 10kbps data rate. Since time-of-flight measurements are performed using the radio data communication, the radio data rate becomes a key parameter, as the ranging clock for standard ranging measurements. Strong signal conditions here refer to a Bit Error Rate (BER) 10^{-5} or lower while worst case conditions refer to a BER of 10^{-4}. In addition to this study, previously, Foster et al. [144] performed range measurements from orbit using a communication radio, using this system between a satellite and a ground station, and obtaining a 1σ error of 650 m for each range observation.

4.2.3. Hybrid measurements

Hybrid methods combine time measurements with phase measurements. Telemetry ranging, for example, has been proposed in [145] as an alternative to conventional two-way ranging. In this method, the ranging signal on the uplink is not re-transmitted through the downlink but telemetry alone modulates the downlink carrier. Basically, telemetry frames provide the timing information needed on the downlink to estimate the round trip light time: successive telemetry frames report directly uplink signal phase measurements. By using the uplink phase and the reception time tag, ranging measurements are generated in a simple way while only using a digital transmission [116,145]. This technique is related to data rate and it gives an order of magnitude better ranging jitter performance than conventional methods at data rates of 1 Mbps or more [146].

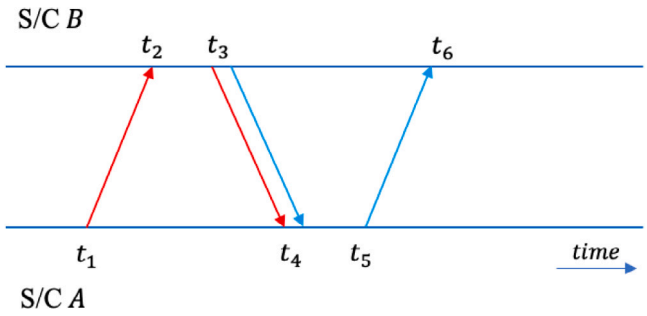

Fig. 10. Illustration of time-derived ranging method.

In addition to ranging, line-of-sight direction can also be measured. Most of the times, small satellites have more than one receiving antenna and, in this specific case, the incoming signal direction can be estimated. Time delay or phase shift can be used between a signal received by the two antennas attached on a baseline at a certain distance. On small satellites, due to size constraints, antenna baseline is often shorter than the wavelength, simplifying the calculations as wavelength ambiguity is eliminated. A third antenna is required in case for 2-axis Line-of-sight direction estimation is needed.

4.2.4. Measurement accuracy

The accuracy of radiometric measurements depends on various factors and it is affected by both random and systematic errors. This section provides an overview of these factors and errors that may affect the measurement accuracy. The investigation is limited to the methods already presented in this paper and used by the missions in Appendix.

In general, the conventional ranging process can be either regenerative or transparent/non-regenerative: in the former case, the spacecraft demodulates and acquires the ranging code with a local replica from the uplink ranging signal and regenerates the ranging code on the downlink, while in the latter the spacecraft translates the uplink ranging signal to the downlink one without code acquisition [147]. In both cases the receiver locks onto the range clock which is the highest frequency of Tone/PN component determining the range resolution. At this stage, thermal noise affects range measurements: this random error is introduced when the received ranging signal is correlated against the local replica of the ranging signal [147]. Basically, the clock tracking jitter due to thermal noise determines the standard deviation of the measurement error. In addition, thermal noise effects the probability of acquisition of a range measurement and it may cause the measurement to fail [136,147]. For both methods, a minimum required integration time can be calculated for a given range measurement error and a given probability of acquisition [148]. In general, Pseudo-noise ranging has a big performance advantage over tones because more measurements can be made with PN in a given measurement period [136]. One-way ranging performance using PN can be given considering a PN square-wave shaped ranging signal and a chip tracking loop as [147]:

$$\sigma_{\rho_{PN}} = \frac{c}{8 f_{rc}} \sqrt{\frac{B_L}{(P_{RC}/N_0)}} \tag{2}$$

with c the speed of light, f_{rc} the frequency of the ranging clock component, B_L one-sided loop noise bandwidth, P_{RC} power of the ranging clock component, N_0 one-side noise power spectral density. End-to-End performance can be calculated via $\sigma_{\rho_{PN}} = \sqrt{(\sigma_{\rho_{PNU}})^2 + (\sigma_{\rho_{PND}})^2}$. Here, $\sigma_{\rho_{PNU}}$ and $\sigma_{\rho_{PND}}$ represent uplink and downlink sides respectively.

Small satellites often lack radio links with coherent tracking, where the downlink carrier is phase-coherent with the received uplink carrier:

this is usually happening for small satellite missions which do not require high accuracy in ranging. In these cases, there might be a chip rate mismatch between the received Tone/PN code and the local replica due to uncompensated Doppler [147], leading to a bias in measurements:

$$\rho_{\text{bias}} = \frac{c\Delta f_{chip} T}{4 f_{chip}} \tag{3}$$

with T integration time, and Δf_{chip} the difference in frequency between the received chip rate and the local chip rate. Accuracy is thus improved by selecting the shortest integration time allowed by the thermal noise constraint in the non-coherent operations [136,147,149]. Considering systematic effects, a group delay calibration process is also generally required to avoid that this masks media effects and errors of solar system ephemeris.

It is also essential to consider that the selected frequency band affects measurement accuracy. Higher frequencies also allow a wide bandwidth usage, due to the larger available spectrum, and this can influence the final system accuracy. Antenna gain and size depend on the operational frequency as well, leading often to better link budgets for higher frequencies, given a certain antenna size [150]. Higher communication speeds are then beneficial for telemetry-based ranging and time-derived ranging techniques. Telemetry-based ranging with the symbol tracking loop and the 2-arm correlator methods performs better than conventional ranging at data rates of 250 kbps and 15 kbps respectively [146]. This is showing why attention has only recently been shifting to these techniques. Assuming a square wave uplink range clock and BPSK-modulated data, the range jitter performance of the telemetry-based ranging (based on the correlator method) can be given as [146]:

$$\sigma_{\rho_{TM}} = \left(1 - \frac{2v}{c}\right)\left(\frac{4\,c\,T_{sd}^2}{\pi\,T_l\,E_S/N_0} + \frac{c}{8 f_{rc}}\sqrt{\frac{B_L}{(P_{RC}/N_0)}}\right) \tag{4}$$

with v the relative velocity, c the speed of light, T_{sd} the channel symbol duration, T_l the correlator integration time and E_S/N_0 the code symbol-to-noise ratio. If timing is measured in units of telemetry/telecommand symbols, instead of directly in seconds, the downlink equation given in Eq. (4) of the telemetry-based ranging could be used for both link sides. Based on the same assumptions used in Eq. (4), and assuming T_l, E_S/N_0 are the same for both downlink and uplink sides, the time-derived ranging error becomes:

$$\sigma_{\rho_{TD}} = \left(1 - \frac{2v}{c}\right)\left(\frac{4\,c\,\sqrt{T_{sd\,U}^4 + T_{sd\,D}^4}}{\pi\,T_l\,E_S/N_0}\right) \tag{5}$$

where $T_{sd\,U}$ and $T_{sd\,D}$ are the symbol duration for uplink and downlink respectively. In fact, the time-derived method has a limited performance because in general the uplink data rate is much lower than downlink one.

Another radiometric data used for the OD process via the ISL is Doppler/Range-rate which could be used to improve ranging accuracy. This observation type is also affected by both random (instrumental and propagation noise) and systematic errors [149]. [151] mentions that systematic errors are at a negligible level in current Doppler tracking systems while numerical propagation noise can sometimes have a non-negligible effect. Moreover, Sun-Earth-Probe (SEP) angles are the strongest disturbance on the carrier frequency stability due to inter-planetary plasma: this noise source can anyway be calibrated, as in the Cassini mission, with a multi-frequency radio system [151]. Tropospheric effects are also another noise source for ground-based measurements which would not affect deep space crosslink RTLT measurements, together with mechanical and thermal noise on antennas (down to a level of 0.005 mm/s with an integration time τ of 60 s [151]).

Measurement error for two-way coherent Doppler due to thermal noise can be approximated by [136]:

$$\sigma_V = \frac{c}{2\sqrt{2}\pi f_c T}\sqrt{\frac{1}{\rho_L} + \frac{G^2 B_L}{(P_C/N_0)}} \tag{6}$$

where f_c the downlink carrier frequency, P_C/N_0 uplink carrier power to noise spectral density ratio, ρ_L the downlink carrier loop signal-to-noise ratio, G the turn-around ratio.

Another most prominent term is the on-board clock stability. When considering one-way measurements, for example, any frequency offset will result in range-rate errors. This problem is completely eliminated with two-way measurements where only one reference (on the measuring side of the communication chain) is used. The accepted stability measure of these frequency standards in the time domain is the two-sample Allan variance with no dead time [152]. Currently, space-qualified oscillators with frequency stability of 10^{-13} [100] are commercially available while current ground-based sources can provide much better performances (better than 10^{-15} at integration time τ of 1000 s [149]). In one of the Europa Clipper piggyback mission proposals, Europa Tomography Probe (ETP) [30], two-way coherent X-band Doppler data from the ISL between Europa Clipper and ETP will be used for ETP's orbit determination process. With the idea that instability appearing at time scales larger than the RTLT could be suppressed by a factor $\pi T/\tau \ll 1$, the quality of the measurements would be achieved with a similar level of accuracy as ground-based systems 0.012 mm/s with an integration time τ of 60 s. Lastly, the computed observables are sensitive to roundoff errors due to finite arithmetic in the computation, also called numerical noise [153]. Based on the Cassini and Juno mission cases, it has been found that [153], numerical errors can be up to 0.06 mm/s with an integration time τ of 60 s.

Based on current technology, several inter-satellite links have been proposed or demonstrated in space. One notable example could be the Rosetta-Philae link, showing two-way communication in S-band up to a distance of 150 km. From the link budget analysis [154], it can be seen that the maximum achievable data rate was 16 kbps. Furthermore, for the constellation missions with a separation of 90 km, a case study on OLFAR is demonstrated the data rate of 48 Mbps [154]. In order to see the impact of inter-satellite distance, a case study for the LUMIO CubeSat showed a data rate of 1.5 kbps for range around 66 000 km. In other words, the specific data rates depend on inter-satellite distance, as shown in Fig. 11 including various transmit powers. Basically, achievable data-rate is limited by inter-satellite distance and measurement accuracy is affected by achievable data-rate. In brief, it can be said that inter-satellite distance indirectly affects measurement accuracy for time-derived methods. Performance comparison of three ranging methods is shown in Fig. 12: conventional PN ranging has the same performance across all the data rates. On the other hand, telemetry-based ranging and time-derived ranging show improved performances with increased data-rate.

4.3. Enabling technologies

This section focuses on the existing systems for inter-satellite radio navigation links and on the analysis of the enabling technologies for future missions. Autonomous radiometric navigation architecture uses the existing communication system required for telecommand, telemetry, and spacecraft navigation. Currently, only two radios are being used for small satellites in deep space: the PROCYON X-band radio and IRIS V2 X-band radio [11]. The X-band radio for PROCYON provides a tone generator for Range and Range Rate (R&RR) and Delta Differential One-Way Range (Δ-DOR) orbit determination with a high-power (15 W) output [155]. On the other hand, the IRIS transponder, developed for MarCO mission by the Jet Propulsion Laboratory, provides sequential/pseudo-noise ranging, Δ-DOR, and Doppler

Table 6
Selected small satellite radios.

	Mass (kg)	Volume (cc)	Frequencies	Max Data Rate	Link
JPL Iris V2.1	1	560	X	6.25 Msps	DTE
General Dynamics SDST	3.2	3386	X/X Ka	30 Msps	DTE
JHU/APL Frontier	2.1	2050	S X Ka	150 Msps	DTE
JHU/APL Frontier Lite	0.4	320	UHF C	10Msps	DTE
JPL UST Lite	3.0	2700	X Ka	300 Msps	DTE
Clyde Space STX	0.08	138	S	2 Mbps	DTE
Tethers Unlimited SWIFT-SLX	0.38	350	S	15 Mbps	DTE
Tethers Unlimited SWIFT-XTS/KTX	0.5	375	X Ka	300 Mbps	DTE
Syrlinks/ EWC27	0.225	207	X	5 Mbps	DTE
Syrlinks/ EWC31	0.25	260	S	2 Mbps	DTE/ISL
Tethers Unlimited SWIFT-RelNav SDR	0.38	350	X	12 Mbps	DTE/ISL
Blue Canyon Technologies SDR	N/A	N/A	UHF S X Ka	100 Mbps	DTE, ISL

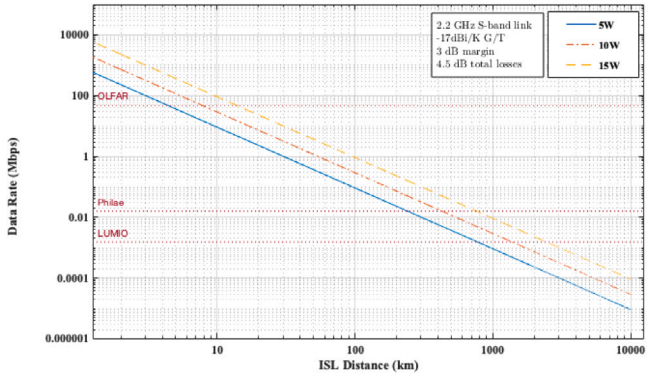

Fig. 11. S-band data rates based on inter-satellite distances at different transmit powers.

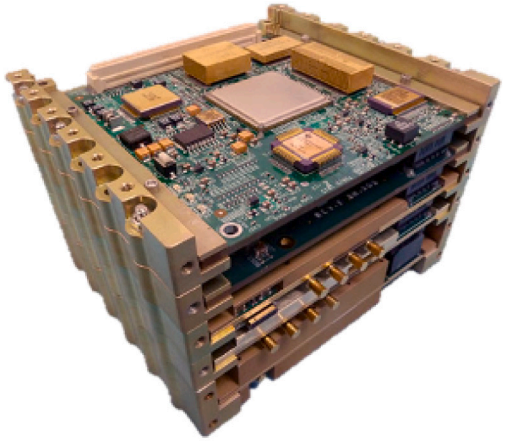

Fig. 13. JPL IRIS V2.1 Transponder [156].

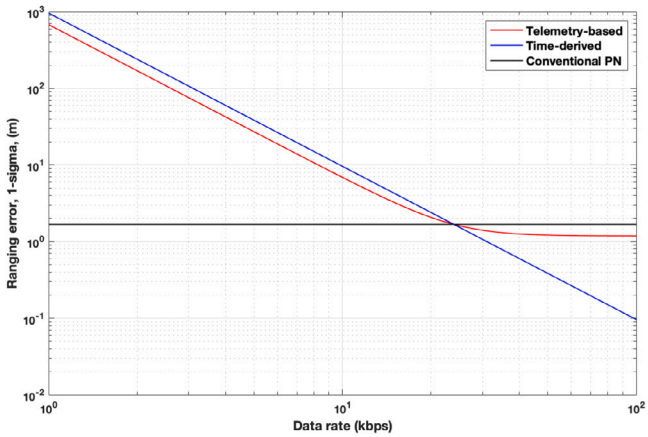

Fig. 12. Performance comparison of various ranging methods.

for navigation purposes with a RF output power of 4 W. Soon, six CubeSats within Artemis-1 mission program; LunaH-Map, Lunar IceCube, Lunar Flashlight, CubeSat for Solar PArticles, BioSentinel, and Near-Earth Asteroid Scout, will be supported by the third generation V2.1 IRIS Transponder [156] (shown in Fig. 13). The latest version of the IRIS V2.1 transponder will provide a communication with distances varies between 1 Mkm and 180 Mkm [157]. Another feature is that maximum downlink data rates up to 6.25 Msps can be supported in BPSK, which is higher than required link performance of Artemis-1 CubeSats, < 256 kbps [157]. It is also expected that proximity operations will be available with this transponder for inter-satellite communication purposes [158]. Regarding transponders for Artemis-1 CubeSats except IRIS, OMOTENASHI will use a new X-band transponder which is developed based on the transponder for the PROCYON spacecraft [159]. This X-band transponder will provide ranging, Doppler measurement, Δ-DOR features for orbit determination. Also, there will be a P-band transceiver on the CubeSat for amateur antennas [159]. Another CubeSat mission in Artemis-1 is CU-E3. For this mission, High-Rate CubeSat Communication System (HRCCS) [160] is designed to demonstrate long-distance, 4 million km, communications [86]. In addition to these, various small satellite radios are considered for cislunar missions in [15].

Regarding others, the Tethers Unlimited SWIFT-RelNav software-defined radio (SDR) system provides crosslink communication and ranging with an accuracy of 10 cm at 12 Mbps data rate based on GPS-like methods [162]. This system works up to 10 km of inter-satellite distance. SDR enables multiple communication modes, such as low-rate data communication around 400 kbps for ranging at greater distances. Regarding the flown missions with an inter-satellite link, MASCOT and Hayabusa-2 are communicated with each other at UHF band, with a mass of less than 100 g Parent-COM (PCOM) transceiver on MASCOT [163]. The data transmission has been performed at 37 kbps. In the PRISMA mission, ISL data transmission and ranging measurement with an accuracy close to 1 cm have been validated. Currently, CNES is developing the next generation of miniaturized ISL for exploration missions, taking into account the previous missions, including PRISMA, feedbacks [163]. For this development, Syrlinks S-band transponder will be used as a hardware baseline. The targeted ranging accuracy shall be below 10 m at 2 sigmas within the ranging algorithm of sequential tone (ESA 100 K). The ranging smoothing techniques will also be used to improve accuracy. For the data transmission performances, 128 kbps is targeted with a maximum of 512 kbps. Another critical development will be to communicate simultaneously with the multiple small satellites in order words multi-point ISL. In the study [163], the Orbiter-Lander link budget is also given as a reference for 100 km mean inter-satellite distance. In the Juventas mission, up to 460 kbps inter-satellite data rate is expected in the S-band frequency with 2 W of RF

Table A.7
List of all studied small satellite missions.

Mission ID	Size	Organization	Destination	Objectives	Ref.
Lunar IceCube	6U	Morehead State University	Cislunar	Search for water on the Moon from a low-perigee highly inclined lunar orbit	[49]
LunaH-Map	6U	Arizona State University	Cislunar	Search for hydrogen on the permanently shadowed lunar crates	[52]
Lunar Flashlight	6U	NASA Jet Propulsion Lab. and Marshall Space Flight Center	Cislunar	Search for ice deposits and identifying favorable locations	[21]
NEA Scout	6U	NASA Jet Propulsion Lab. and Marshall Space Flight Center	Small Bodies	Take pictures of the asteroid 1991 VG and observe its position in space using a solar sail propulsion	[21]
CuSP	6U	Southwest Research Institute	Lunar Flyby	Study dynamic particles and magnetic fields in near-Earth orbit, and support space weather research	[84]
LunIR	6U	Lockheed Martin	Cislunar	Perform a lunar flyby taking images of the lunar surface and its environment for remote sensing, site selection observations, and to surface characterization	[54]
OMOTENASHI	6U	JAXA, University of Tokyo	Cislunar	Demonstrate a lunar semi-hard landing by a CubeSat and observe the radiation environment and soil mechanics	[58]
EQUULEUS	6U	JAXA, University of Tokyo	Cislunar	Demonstrate trajectory control techniques, and to observe the Moon from Earth–Moon L2	[62]
BioSentinel	6U	NASA Ames Research Center	Lunar Flyby	Measure the impact of space radiation on living organisms over long duration	[85]
ArgoMoon	6U	Argotec, Italian Space Agency	Cislunar	Taking pictures of the SLS secondary propulsion stage and the Moon and the surrounding environment	[56]
Cislunar Explorers	6U	Cornell University	Cislunar	Demonstrate the water electrolysis propulsion and autonomous optical navigation technologies	[14,60]
CU-E3	6U	University of Colorado	Lunar Flyby	Demonstrate long-distance (more than 4 million km) communications	[86]
Team Miles	6U	Team Miles Tampa Hackerspace	Lunar Flyby	Demonstrate long-distance communications with a software-defined radio operating in the S-band and navigation capability using plasma thrusters	[87,88]
M-ARGO	12U	ESA	Small Bodies	Rendezvous with an asteroid, characterize its physical properties and assess potential for resource exploitation	[31]
HALO	6U	NASA Glenn Research Center	Cislunar	Survey the surface of the Moon and to observe the impinging solar wind and the reflected ion component	[24]
DAVID	6U	NASA Glenn Research Center	Small Bodies	investigate an asteroid, 2001 GP2, which is the smallest asteroid investigated by previous missions	[25]
MAT	Mid ESPA	Space Science Institute, Exo Terra Resource, Malin Space Science Systems, NASA GSFC, CNRS/LMD	Mars	Observe the temporal evolution of dust storms and water ice clouds and to detect changes in surface physical properties throughout the diurnal cycle	[23,51]
CUVE	12U	University of Maryland, NASA GSFC	Venus	Measure the ultraviolet light absorption to understand the Venus atmospheric dynamics	[23,71]

(*continued on next page*)

power and estimated measurement accuracies between HERA maincraft are 1 m in range and 1 mm/s in range-rate [47].

There are also small radios flown on larger spacecraft. These are typically more volume consuming radios which still can be useful for smaller satellites. Regarding those, the Small Deep-Space Transponder (SDST) has been flown on multiple deep space missions such as Deep Space 1, Deep Impact, and InSight [164]. Frontier, Universal Space Transponder (UST), Universal Space Transponder (UST)-lite are other examples of such small transponders [165,166]. Typically, Frontier consumes less power (9.7 W) than others 17.9 W (SDST), 45 W (UST), and 30 W (UST-lite) [167]. At 20 Hz loop bandwidth, receiver sensitivities are −151 dBm for SDST and −160 dBm for others. From the data rate perspective, UST, UST-lite support up to 300 Msps for downlink and 37.5 Msps for uplink. In case for Frontier and SDST, telemetry rates are up to 150 Msps, 30 Msps and telecommand rates are up to 1 Msps, 4 ksps respectively. In Table 6, selected small satellite radios can be seen.

Table A.7 (*continued*).

Mission ID	Size	Organization	Destination	Objectives	Ref.
JUMPER	N/A	Southwest Research Institute NASA JPL, CU LASP	Jupiter	Understand the solar wind's interaction with Jupiter's magnetosphere and to determine its energetic neutral atom emissions	[23,81]
PrOVE	Mid ESPA	University of Maryland, NASA GSFC, JPL	Small Bodies	Perform a close flyby of a new and Jupiter familycomet and study surface structure and volatile inventory	[23,79]
Ross	12U	Lockheed Martin, Uni. of Hawaii, Malin Space Science Systems, SETI Institute	Small Bodies	Obtain fundamental data on size, shape and structure during flyby to different Near Earth Objects	[23,73]
VAMOS	ESPA	NASA Jet Propulsion Lab., Uni. of Illinois, Uni. of Michigan, CNES, DLR	Venus	Determine the global seismic activity of Venus	[23,82]
WATER	ESPA	John Hopkins Applied Physics Laboratory, NASA GRC, GSFC, MSFC	Cislunar	Characterize water on the surface of the Moon including its chemical form, and distribution	[23,67]
CubeX	36U	Smithsonian Astrophysical Observatory, Harvard Uni., MIT, Carnegie Inst., of Washington., GSFC, Birkbeck College, Uni. of Arizona, NASA Ames RS	Cislunar	Identify and spatially map lunar crust and demonstrate semi-autonomous deep space navigation using X-ray pulsars with a X-ray telescope	[23,72]
IMPEL	ESPA	NASA Johnson Space Center	Cislunar	Explore a site of potentially recent volcanism on the Moon	[23,69]
MARIO	16U	Politecnico di Milano	Mars	Perform thermal radiation imaging and to establish long-distance X-band communication link with the Earth	[53]
ASPECT	3U	VTT, University of Helsinki, Aalto University, ESA	Small Bodies	Spectral imaging of Didymos before and after impact	[32]
DustCube	3U	University of Vigo, University of Bologna, MICOS, ESA	Small Bodies	Characterize the natural dust environment and ejected plume due to high speed impact on the asteroid and imaging of the Didymoon before, during and after impact	[33]
CUBATA	3U	GMV, University of La Sapienza, INTA, ESA	Small Bodies	Determine the gravity field of the Didymos before and after impact with Doppler shift provided due to the relative line-of-sight velocity between the two spacecraft and to observe the impact from two different viewpoints	[34]
PALS	3U	Swedish Institute of Space Physics, KTH, DLR, IEEC, AAC Microtec, ESA	Small Bodies	Characterize surface structure and magnetization, and observe impact plume	[35]
AGEX	3U	ROB, ISAE Supaero, Emxys, Antwerp Space, ESA	Small Bodies	Measure mass during the descent and landing, and determination of dynamical state, local gravity before and after impact	[36]

(*continued on next page*)

5. Perspectives for autonomy

This paper showed that small satellites are receiving increasing attention for deep space missions and that satellite formations are being proposed to address several scientific missions. Satellite miniaturization has been used often to lower mission costs but, for the specific case of deep space nano-satellites, the operational cost would not scale as well due to the requirement of having a full flight dynamics team for navigation, exactly as for a much bigger spacecraft. Autonomous navigation can help lower this requirement and several techniques have been proposed (as described in Section 3). Optical and X-ray pulsar very suited for mission where a single satellite is present while crosslink radiometric navigation is very suited for satellite formations, as shown in Section 4.

Autonomy, in the sense of not being tied to a ground operations team and a ground station can bring several advantages for a deep space mission: the most obvious one is that orbit determination and correction maneuvers could be calculated on-board and updated without considering eventual visibility issues (due to distance or power limitations but also during a solar conjunction). This comes as a definite advantage for missions to distant locations where the Earth might not be in view at the time the trajectory needs to be re-calculated, opening up a big amount of possibilities. Techniques like Terrain Relative Navigation (as described in Section 3.1.1) can greatly increase mission performances providing a much higher accuracy that could be available with ground-based measurements. In a similar way, autonomous crosslink navigation could serve as a navigation provider to other spacecraft in a highly asymmetrical gravity field such as CAPSTONE mission is aiming at demonstrating in the cislunar vicinity. Similar techniques could be applied to small bodies missions, such as comets or asteroid fly-bys, where a full satellite swarm could be used, instead of a single spacecraft (as, for example in the Comet Interceptor mission [63,64]).

6. Conclusion

This study presented an overview of the recent scientific and technological advances in navigation systems and techniques for deep space small satellites, with a focus on autonomy as an enabler for more capable missions. Current trends have been derived from a total of 64 proposed deep space small satellite missions with the most popular destinations being the cislunar space and small bodies. From the survey,

Table A.7 (*continued*).

Mission ID	Size	Organization	Destination	Objectives	Ref.
Juventas	6U	GMV, Astronika, Brno University, CSRC, ESA	Small Bodies	Characterize the gravity field and internal structure and to determine the surface and the dynamical properties of Didymos	[37,47]
MILANI	6U	IRF, KTH, RSL, Aalto Uni. VTT Research Center, Uni. of Helsinki, DLR Bremen, SSC, ESA	Small Bodies	Map the surface composition and internal structure of Didymos	[37,50]
LUMIO	12U	Politecnico di Milano, TU Delft, EPFL, S&T Norway, Leonardo S.p.A, ESA	Cislunar	Observe, quantify and characterize meteroid impacts on the Lunar farside by detecting their impact flashes with an optical camera	[31,38]
VMMO	12U	MPB Communications, University of Surrey, Lends R&D, University of Winnipeg, ESA	Cislunar	Search for water ice deposits in permanently shadowed craters at the south pole	[31,41]
MoonCare	12U	Von Karman Institute, DLR, Tyvak International, Politecnico di Torino	Cislunar	Characterize and study the lunar radiation and its effect on microorganisms	[31,39]
CLE	12U	ISIS bv, ASTRON, Radboud Uni. Nijmegen, Uni. Twente, TU Delft	Cislunar	Demonstrate radio astronomy below 30MHz in lunar radio quiet zone	[31,40]
Cupid's Arrow	Pr.	NASA Jet Propulsion Lab., CalTech, Georgia Tech., Uni. Nancy	Venus	Measure noble gases in Venus' Atmosphere	[23,66]
SAEVe	Pr.	NASA Glenn Research Center, Imperial College London, Wesleyan Uni., Lunar and Planetary Institute NASA JPL, Uni. of Oxford	Venus	Determine geophysical activity of Venus	[23,75]
SNAP	Pr.	Hampton University, NASA Langley RC, JPL, Uni. of California Berkeley, Purdue Uni.	Uranus	Examine the physical and chemical processes in the Uranus atmosphere	[23,68]
Mini-Maggie	3U	University of Alaska, NASA Jet Propulsion Lab.	Europa	Characterize the magnetic field and gravity around Europa	[27]
DARCSIDE	3U	New Mexico State University	Europa	Perform singlelow-altitude pass above Europa and measure atmospheric density and heavy ion flux	[28]
Sylph	Pr.	Cornell University	Europa	Sample a presumed plume on Europa by performing single 2km altitude flyby above the surface	[29]
ETP	Pr.	Italian Space Agency	Europa	Measure the magnetic field at different orbital and rotational frequencies, rotational state and tidal information with an inter-satellite link enabled by a transponder	[29,30]
B1	Pr.	JAXA	Small Bodies	Encounter and fly closer to take a multi-dimensional picture of the comet	[63,64]
B2	Pr.	ESA	Small Bodies	Encounter and fly closer to take a multi-dimensional picture of the comet	[63,64]
BIRDY-T	3U	Paris Observatory CERES, Uni. PSL, Odysseus Space SA	Small Bodies	Fly small solar system body to observe the size and shape and perform radio science experiment with an inter-satellite link between a mother-spacecraft and the CubeSat	[7]
AI3	16U	Uni. of Kiel, Max Planck Institute for Solar System Research	Small Bodies	Characterize of an asteroid, by making use of inter-satellite link, and detect the seismic wave after an impactevent produced by an impactor,	[70]

(*continued on next page*)

it can be clearly seen that the far majority of the missions is relying primarily on ground-based navigation techniques while only in few cases navigation autonomy has been selected. This paper also presented several deep space navigation techniques suited for satellite formations, in particular optical, X-ray pulsar and crosslink radiometric together with their basic working principles and the most common error sources. Crosslink radiometric navigation has been further studied including measurement methods and instruments in use. This method comes with a main advantage of using existing communication systems, such that existing missions can benefit from this technique with minimal changes. An autonomous navigation technique, LiAISON, has been shown to achieve an accuracy in the order of tens to hundreds of meters and millimeters per second for position and velocity for fully autonomous missions around small bodies and in the cislunar space. By analyzing the mission survey results, this paper showed that more than half of the presented missions, 58%, uses inter-satellite communication and most of them, 81%, would benefit from autonomous radio-navigation. This would bring several advantages: by lowering the distance over which navigation measurements are carried out, the required accuracy and complexity can be reduced. This brings a great simplification to the mission, reducing its cost and size. Autonomy, furthermore, can enable new missions by allowing to perform navigation also in mission phases where the Earth is not directly reachable (due to its distance or lack of visibility). Overall, this paper showed that autonomous navigation

Table A.7 (*continued*).

Mission ID	Size	Organization	Destination	Objectives	Ref.
MarsDrop	Pr.	NASA JPL, Aerospace Corporation, Planetary Science Institute	Mars	Take instruments to difficult sites inaccessible for large landers and rovers	[48]
NanoSWARM	3U	Uni. of California Santa Cruz UCLA, MIT, UC Berkeley, APL, Ames, JPL, Tyvak, KASI Northrop Grumman	Cislunar	Understand mechanisms of space weathering, near surface water formation and the origin of planetary magnetism	[76]
MarCO	6U	NASA Jet Propulsion Lab.	Mars	Fly independently to Mars and act as a relay during InSight's entry, descent and landing phase	[19,55,161]
MISEN	Mid ESPA	UC Berkeley SSL, UCLA ESS, Tyvak LLC, Advanced Space LLC	Mars	Characterize the magnitude, global patterns and real-time response to space weather of ion escape at Mars	[23,61]
MiLuV	ESPA	NASA Goddard Space Flight Center	Cislunar	Map lunar volatiles by using a lunar ice spectrometer	[23,78]
APEX	Pr.	Johns Hopkins Uni., Arizona State Uni., Sandia National Lab., Uni. Maryland	Small Bodies	Determine the interior structure of an asteroid, Apophis, to understand its origin and evolution	[23,74]
PRISM	12U	NASA GSFC, Morehead St. Uni., JHU APL, Uni. of Iowa, Georgia Institute of Tech., NASA JPL	Small Bodies	Investigate Phobos with an ion mass spectrometer	[23,77]
Aeolus	24U	NASA Ames Research Center	Mars	Produce global wind speed map, determine the global energy balance and measure atmospheric aerosol at Mars	[23,59]
BOLAS	12U	NASA GSFC, Morehead State Uni., Tethers Unlimited, Busek	Cislunar	Investigate the hydration and space weathering processes at the Moon	[23,80]
OLFAR	N/A	ASTRON	Cislunar	Investigate frequency ranges between 30 kHz - 30 MHz at Lunar orbit or Sun–Earth L4-L5	[42]
DSL	N/A	Radboud University Nijmegen, CAS-SHAO	Cislunar	Explore frequency range between 100 KHz - 50 MHz at Sun–Earth L2 with 8 spacecrafts	[43]
DEx	N/A	Radboud University Nijmegen	Sun–Earth L2	Investigate frequency ranges between 100 KHz - 80MHz and 1MHz-100MHz respectively at Sun–Earth L2	[44]
SULFRO	2U	Shanghai Engineering Centre for Microsatellites	Sun–Earth L2	Investigate frequency ranges between 100 KHz - 80 MHz and 1 MHz-100 MHz respectively at Sun–Earth L2	[45]
MIIAR	6U	North South University	Mars	Study of Mars surface using hyperspectral imaging and act as relay satellites between surface assets and the Earth	[65]
MMO	6U	Malin Space Science Systems	Mars	Measure the Mars atmosphere in visible and infrared wavelengths from Mars orbit and serve as a relay for Mars surface based missions	[57]
CAPSTONE	12U	Advanced Space	Cislunar	Demonstrate the reliability of innovative spacecraft-to-spacecraft navigation solutions as well as communication capabilities with Earth	[83]

techniques can be applied to current and planned deep space satellite formation missions.

Declaration of competing interest

The authors declare that they have no known competing financial interests or personal relationships that could have appeared to influence the work reported in this paper.

Appendix

In the previous sections, mission objectives have not been given. This section, on the other hand, shows the further details about the missions analyzed in this study. Following list, see Table A.7, contains their name, volume, leading organizations, destinations, primary objectives and corresponding references.

References

[1] M. Sweeting, Modern small satellites-changing the economics of space, Proc. IEEE 106 (3) (2018) 343–361.

[2] Z.J. Towfic, D. Heckman, D. Morabito, R. Rogalin, C. Okino, D.S. Abraham, Simulation and analysis of opportunistic MSPA for multiple cubesat deployments, in: 15th International Conference on Space Operations, American Institute of Aeronautics and Astronautics, 2018, http://dx.doi.org/10.2514/6.2018-2396.

[3] S. Bhaskaran, J.E. Riedel, S.P. Synnott, Autonomous optical navigation for interplanetary missions, in: Space Sciencecraft Control and Tracking in the New Millennium, Vol. 2810, International Society for Optics and Photonics, 1996, pp. 32–43.

[4] J. Riedel, S. Bhaskaran, S. Desai, D. Han, B. Kennedy, T. McElrath, G. Null, M. Ryne, S. Synnott, T. Wang, et al., Using autonomous navigation for interplanetary missions: The validation of deep space 1 AutoNav, 2000.

[5] M. Chory, D. Hoffman, J. LeMay, Satellite autonomous navigation-status and history, Pln, 1986, pp. 110–121.

[6] V. Franzese, P.D. Lizia, F. Topputo, Autonomous optical navigation for LUMIO mission, in: 2018 Space Flight Mechanics Meeting, American Institute of Aeronautics and Astronautics, 2018, http://dx.doi.org/10.2514/6.2018-1977.

[7] D. Hestroffer, M. Agnan, B. Segret, G. Quinsac, J. Vannitsen, P. Rosenblatt, J. Miau, BIRDY-interplanetary CubeSat for planetary geodesy of small solar system bodies (SSSB), in: AGU Fall Meeting Abstracts, 2017.

[8] K.A. Hill, Autonomous Navigation in Libration Point Orbits (Ph.D. thesis), University of Colorado, 2007.

[9] A.R. Dahir, Lost in Space: Autonomous Deep Space Navigation (Ph.D. thesis), University of Colorado at Boulder, 2020.

[10] A. Poghosyan, A. Golkar, Cubesat evolution: Analyzing CubeSat capabilities for conducting science missions, Prog. Aerosp. Sci. 88 (2017) 59–83.

[11] S. Papais, B.J. Hockman, S. Bandyopadhyay, R.R. Karimi, S. Bhaskaran, I.A. Nesnas, Architecture trades for accessing small bodies with an autonomous small spacecraft, in: 2020 IEEE Aerospace Conference, IEEE, 2020, pp. 1–20.

[12] A. Freeman, Deep Space Nanosats-Positioned for Exponential Growth, Jet Propulsion Laboratory, National Aeronautics and Space ..., Pasadena, CA, 2016.

[13] A. Freeman, Exploring our solar system with CubeSats and SmallSats: the dawn of a new era, CEAS Space J. 12 (4) (2020) 491–502, http://dx.doi.org/10.1007/s12567-020-00298-5.

[14] P. Clark, Cubesats in cislunar space, 2018.

[15] S. Schaire, Y. Wong, G. Bussey, M. Shelton, D. Folta, C. Gramling, P. Celeste, M. Anderson, T. Perrotto, B. Malphrus, et al., Lunar and Lagrangian point L1/L2 CubeSat communication and navigation considerations, 2017.

[16] R. Funase, T. Inamori, S. Ikari, N. Ozaki, S. Nakajima, H. Koizumi, A. Tomiki, Y. Kobayashi, Y. Kawakatsu, One-year deep space flight result of the world's first full-scale 50kg-class deep space probe PROCYON and its future perspective, 2016.

[17] Y. Tsuda, M. Yoshikawa, M. Abe, H. Minamino, S. Nakazawa, System design of the hayabusa 2—asteroid sample return mission to 1999 JU3, Acta Astronaut. 91 (2013) 356–362, http://dx.doi.org/10.1016/j.actaastro.2013.06.028.

[18] J. Biele, S. Ulamec, Capabilities of philae, the rosetta lander, in: Origin and Early Evolution of Comet Nuclei, Springer, 2008, pp. 275–289.

[19] S.W. Asmar, S. Matousek, Mars cube one (MarCO) shifting the paradigm in relay deep space operation, in: SpaceOps 2016 Conference, American Institute of Aeronautics and Astronautics, 2016, http://dx.doi.org/10.2514/6.2016-2483.

[20] NASA, What is lunar flashlight? 2020, URL https://www.nasa.gov/directorates/spacetech/small_spacecraft/What_is_Lunar_Flashlight. (Accessed Feb 2021).

[21] NASA, Artemis 1 secondary payloads, AES EM-1 secondaries fact sheet, 2015, URL https://www.nasa.gov/sites/default/files/atoms/files/aes-secondaries-fs-v508c.pdf. (Accessed June 2020).

[22] C. Mercer, Planetary science deep space SmallSat studies, in: Lunar Planetary Science Conference Special Session, The Woodlands, Texas, 2018.

[23] C.R. Mercer, Small satellite missions for planetary science, 2019.

[24] NASA, NASA's space cubes: Small satellites provide big payoffs, 2017, URL https://www.nasa.gov/feature/nasa-s-space-cubes-small-satellites-provide-big-payoffs. (Accessed June 2020).

[25] M. Chandrashekhar, Diminutive Asteroid Visitor using Ion Drive (DAVID): A 6U-CubeSat Mission Analysis of a Near Earth Asteroid Visit.

[26] NASA, Europa clipper home page at NASA, 2020, URL https://europa.nasa.gov/mission/about/. (Accessed June 2020).

[27] B. Burgett, J. Long, P. Whaley, A. Raz, R. Herrick, D. Thorsen, P. Delamere, Mini-MAGGIE: CubeSat magnetism and gravity investigation at europa, in: Lunar and Planetary Science Conference, Vol. 47, 2016, p. 1928.

[28] A.E. Thelen, N. Chanover, J. Murphy, K. Rankin, S. Stochaj, A europa CubeSat concept study for measuring atmospheric density and heavy ion flux, J. Small Satell. 6 (2017) 591–607.

[29] T. Imken, B. Sherwood, J. Elliott, A. Frick, K. McCoy, D. Oh, P. Kahn, A. Karapetian, R. Polit-Casillas, M. Cable, et al., Sylph-a SmallSat Probe Concept Engineered to Answer Europa's Big Question, Jet Propulsion Laboratory, National Aeronautics and Space ..., Pasadena, CA, 2016.

[30] M. Di Benedetto, L. Imperi, D. Durante, M. Dougherty, L. Iess, V. Notaro, P. Racioppa, Augmenting NASA europa clipper by a small probe: Europa tomography probe (ETP) mission concept, 2016.

[31] R. Walker, D. Binns, C. Bramanti, M. Casasco, P. Concari, D. Izzo, D. Feili, P. Fernandez, J.G. Fernandez, P. Hager, D. Koschny, V. Pesquita, N. Wallace, I. Carnelli, M. Khan, M. Scoubeau, D. Taubert, Deep-space CubeSats: thinking inside the box, Astron. Geophys. 59 (5) (2018) 524–530, http://dx.doi.org/10.1093/astrogeo/aty232.

[32] T. Kohout, A. Näsilä, T. Tikka, M. Granvik, A. Kestilä, A. Penttilä, J. Kuhno, K. Muinonen, K. Viherkanto, E. Kallio, Feasibility of asteroid exploration using CubeSats—ASPECT case study, Adv. Space Res. 62 (8) (2018) 2239–2244.

[33] F. Perez, D. Modenini, A. Vázquez, F. Aguado, R. Tubío, G. Dolgos, P. Tortora, A. Gonzalez, R.L. Manghi, M. Zannoni, et al., Dustcube, a nanosatellite mission to binary asteroid 65803 didymos as part of the ESA AIM mission, Adv. Space Res. 62 (12) (2018) 3335–3356.

[34] GMV, AIM industry days, CUBATA, cubesat at target asteroid, 2016, URL https://indico.esa.int/event/133/contributions/765/attachments/817/994/10_CUBATA.pdf. (Accessed June 2020).

[35] E. Vinterhav, AIM/PALS AIM Industry Days, URL https://indico.esa.int/event/133/contributions/762/attachments/847/1025/08_PALS.pdf.

[36] O. Karatekin, The asteroid geophysical explorer (AGEX); a proposal to explore didymos system using cubesats, in: 41st COSPAR Scientific Assembly, Vol. 41, 2016.

[37] P. Tortora, M. Zannoni, G. Gutierrez, P. Martino, I. Carnelli, Didymos Gravity Science through Juventas Satellite-to-Satellite Doppler Tracking.

[38] S. Speretta, F. Topputo, J. Biggs, P.D. Lizia, M. Massari, K. Mani, D.D. Tos, S. Ceccherini, V. Franzese, A. Cervone, P. Sundaramoorthy, R. Noomen, S. Mestry, A. do Carmo Cipriano, A. Ivanov, D. Labate, L. Tommasi, A. Jochemsen, J. Gailis, R. Furfaro, V. Reddy, J. Vennekens, R. Walker, LUMIO: achieving autonomous operations for lunar exploration with a CubeSat, in: 2018 SpaceOps Conference, American Institute of Aeronautics and Astronautics, 2018, http://dx.doi.org/10.2514/6.2018-2599.

[39] C. Conigliaro, D. Calvi, L. Franchi, F. Stesina, S. Corpino, Design and analysis of an innovative cubesat thermal control system for biological experiment in lunar environment, in: Proceedings of the 69th International Astronautical Congress, Bremen, Germany, 2018, pp. 1–5.

[40] M. Bentum, A.-J. Boonstra, M. Klein Wolt, C. Brinkerink, N. Alpay Koc, S. Fuster, R. Kumar, D. Prinsloo, C. Verhoeven, M. Verma, The CubeSat low frequency explorer (CLE) in lunar orbit, in: 42nd COSPAR Scientific Assembly, 42, 2018.

[41] R. Kruzelecky, P. Murzionak, J. Lavoie, I. Sinclair, G. Schinn, C. Underwood, Y. Gao, C. Bridges, R. Armellin, A. Luccafabris, et al., VMMO lunar volatile and mineralogy mapping orbiter, in: 48th International Conference on Environmental Systems, 2018.

[42] R.T. Rajan, S. Engelen, M. Bentum, C. Verhoeven, Orbiting low frequency array for radio astronomy, in: 2011 Aerospace Conference, IEEE, 2011, pp. 1–11.

[43] X. Chen, J. Burns, L. Koopmans, H. Rothkaehi, J. Silk, J. Wu, A.-J. Boonstra, B. Cecconi, C.H. Chiang, L. Chen, et al., Discovering the sky at the longest wavelengths with small satellite constellations, 2019, arXiv preprint arXiv:1907.10853.

[44] D. Spokesperson, M.K. Wolt, A White paper for a low–frequency radio interferometer mission to explore the cosmological Dark Ages for the L2, L3 ESA Cosmic Vision program.

[45] S. Wu, W. Chen, Y. Zhang, W. Baan, T. An, SULFRO: a swarm of nano-/micro-satellite at SE L2 for space ultra-low frequency radio observatory, 2014.

[46] R. Walker, D. Koschny, C. Bramanti, I. Carnelli, E.C.S. Team, et al., Miniaturised asteroid remote geophysical observer (M-ARGO): a stand-alone deep space CubeSat system for low-cost science and exploration missions, in: 6th Interplanetary CubeSat Workshop, Vol. 30, No. 05, Cambridge, UK, 2017.

[47] H. Goldberg, O. Karatekin, B. Ritter, A. Herique, P. Tortora, C. Prioroc, B.G. Gutierrez, P. Martino, I. Carnelli, B. Garcia, The juventas CubeSat in support of ESA's hera mission to the asteroid didymos, 2019.

[48] R.L. Staehle, S. Spangelo, M.S. Lane, K.M. Aaron, R. Bhartia, J.S. Boland, L.E. Christensen, S. Forouhar, M. de la Torre Juarez, N. Trawny, et al., Multiplying mars lander opportunities with marsdrop microlanders, 2015.

[49] B.K. Malphrus, K.Z. Brown, J. Garcia, C. Conner, J. Kruth, M.S. Combs, N. Fite, S. McNeil, S. Wilczweski, K. Haught, A. Zucherman, P. Clark, K. Angkasa, N. Richard, T. Hurford, D. Folta, C. Brambora, R. MacDowall, P. Mason, S. Hur-Diaz, J. Breeden, R. Nakamura, A. Martinez, M.M. Tsay, The lunar IceCube EM-1 mission: Prospecting the moon for water ice, IEEE Aerosp. Electron. Syst. Mag. 34 (4) (2019) 6–14, http://dx.doi.org/10.1109/maes.2019.2909384.

[50] D. Andrews, J.-E. Wahlund, T. Kohout, A. Penttilä, Asteroid prospection explorer (APEX) cubesat for the ESA hera mission, in: EPSC, 2019, 2019, pp. EPSC–DPS2019.

[51] L. Montabone, M. VanWoerkom, B. Cantor, M. Wolff, M. Capderou, F. Forget, M. Smith, Mars aerosol tracker (MAT): an areostationary CubeSat to monitor dust storms and water ice clouds, in: Lunar and Planetary Science Conference, Vol. 49, 2018.

[52] A. Babuscia, K. Angkasa, B. Malphrus, C. Hardgrove, Development of Telecommunications Systems and Ground Support for EM-1 Interplanetary Cubesats Missions: Lunar IceCube and LunaH-Map, Jet Propulsion Laboratory, National Aeronautics and Space ..., Pasadena, CA, 2017.

[53] K.V. Mani, A. Casado, V. Franzese, F. Topputo, A. Cervone, Systems design of MARIO: Stand-alone 16U CubeSat from earth to mars, 2019.

[54] NASA, NASA selects lockheed Martin's LunIR CubeSat for artemis I secondary payload, 2016, URL https://www.nasa.gov/feature/nasa-selects-lockheed-martin-s-lunir-cubesat-for-artemis-i-secondary-payload. (Accessed June 2020).

[55] A.T. Klesh, J. Baker, J. Krajewski, MarCO: Flight review and lessons learned, in: 33rd Annual AIAA/USU Conference on Small Satellites, 2019.

[56] M.V. Di Tana, C. Fiori, S. Simonetti, S. Pirrotta, Argomoon, a multipurpose CubeSat platform for missions in moon vicinity and orbit, in: European Planetary Science Congress, 12, 2018.

[57] J.L. Green, Planetary Science Division Status Report, Tech. rep., NASA, Planetary Science Division, 2015, 2015 URL https://www.hou.usra.edu/meetings/leag2015/presentations/Tuesday/0850-Green.pdf.

[58] S. Campagnola, J. Hernando-Ayuso, K. Kakihara, Y. Kawabata, T. Chikazawa, R. Funase, N. Ozaki, N. Baresi, T. Hashimoto, Y. Kawakatsu, T. Ikenaga, K. Oguri, K. Oshima, Mission analysis for the EM-1 CubeSats EQUULEUS and OMOTENASHI, IEEE Aerosp. Electron. Syst. Mag. 34 (4) (2019) 38–44, http://dx.doi.org/10.1109/maes.2019.2916291.

[59] A. Cook, A. Colaprete, J. Fisher, L.L. Gordley, V. Jha, B. Marshall, D. Guerin, The Doppler wind and thermal sounder instrument for the aeolus mission concept to mars, in: AGUFM, 2019, 2019, pp. P11D–3487.

[60] S.S.D. Studio, Lunar cubesat: "cislunar explorers", 2020, URL https://www.spacecraftresearch.com/lunar-cubesat. (Accessed June 2020).

[61] R. Lillis, S. Curry, D. Larson, C. Russell, D. Brain, D. Curtis, J. Parker, N. Parrish, J. Puig-Suari, Mars ion and sputtering escape network (MISEN), in: 2018 Plantary Science Deep Space SmallSat Mission Concepts Meeting, 2018, pp. 1–19.

[62] K. Oguri, K. Oshima, S. Campagnola, K. Kakihara, N. Ozaki, N. Baresi, Y. Kawakatsu, R. Funase, EQUULEUS trajectory design, J. Astronaut. Sci. (2020) http://dx.doi.org/10.1007/s40295-019-00206-y.

[63] Request for Information for the Provision of Small Spacecraft's for Comet Interceptor, techreport, European Space Research and Technology Centre, 2020.

[64] C.I.P.-. Proposal, Comet Interceptor:A Mission to a Dynamically New Solar System Object, Tech. rep., 2020, URL http://www.cometinterceptor.space/uploads/1/2/3/7/123778284/comet_interceptor_executive_summary.pdf. (Accessed June 2020).

[65] M. Bappy, R. Huq, P. Das, S. Siddique, System design concept of mars intelligent imaging & atmospheric research cubesat constellation using distributed deep learning (miiar), 2019.

[66] C. Sotin, G. Avice, J. Baker, A. Freeman, S. Madzunkov, T. Stevenson, N. Arora, M. Darrach, G. Lightsey, B. Marty, Cupid's arrow: A small satellite concept to measure noble gases in venus' atmosphere, in: Lunar and Planetary Science Conference, Vol. 49, 2018.

[67] C. Hibbitts, B. Clyde, D. Blewett, P. Brandt, L. Burke, B. Cohen, J. Dankanich, D. Hurley, R. Klima, D. Lawrence, et al., The lunar WATER mission: A PSDS3 feasibility study of a solar-electric propulsion small sat mission to characterize the water on the moon, in: Lunar and Planetary Science Conference, Vol. 49, 2018.

[68] K. Sayanagi, R. Dillman, A. Simon, D. Atkinson, M. Wong, T. Spilker, S. Saikia, J. Li, D. Hope, Small next-generation atmospheric probe (SNAP) concept, 2017.

[69] D. Draper, J. Stopar, S. Lawrence, B. Denevi, K. John, L. Graham, J. Hamilton, Z. Fletcher, J. Gruener, S. Bertsch, The irregular mare patch exploration lander (IMPEL) smallsat mission concept, in: Lunar and Planetary Science Conference, Vol. 49, 2018.

[70] J. Deller, E. Vilenius, O. Roders, O. Karatekin, S. Pursiainen, K. Wada, P. Tortora, T. Kohout, P. Bambach, Asteroid in-situ interior investigation-3way: Understanding the formation processes and evolution of small solar system bodies, in: EPSC, 2019, 2019, pp. EPSC–DPS2019.

[71] V. Cottini, S. Aslam, N. Gorius, T. Hewagama, L. Glaze, N. Ignatiev, G. Piccioni, E. D'Aversa, CUVE-cubesat UV experiment: Unveil venus' UV absorber with cubesat UV mapping spectrometer, in: 15th Meeting of the Venus Exploration and Analysis Group (VEXAG), 2061, 2017, p. 8044.

[72] S. Romaine, R. Kraft, K. Gendreau, I. Crawford, L.R. Nittler, D. Kring, J. Hong, N. Petro, J. Mitchell, L. Winternitz, et al., Cubesat X-ray telescope (cubex) for lunar elemental abundance mapping and millisecond X-ray pulsar navigation, in: 42nd COSPAR Scientific Assembly, Vol. 42, 2018.

[73] B. Bierhaus, B. Clark, J. Hopkins, Ross (née, CAESAR), 2018, URL https://www.lpi.usra.edu/sbag/meetings/jan2018/presentations/930-Bierhaus-Ross.pdf. (accessed June 2020).

[74] J. Plescia, O. Barnouin, D. Richardson, N. Schmerr, D. Lawrence, B. Denevi, C. Ernst, H. Yu, The asteroid probe experiment (APEX) mission, 2017.

[75] T. Kremic, et al., Seismic and Atmospheric Exploration of Venus (SAEVe) Final Report, Tech. rep., Lunar and Planetary Institute, 2018.

[76] I. Garrick-Bethell, C. Pieters, C. Russell, B. Weiss, J. Halekas, D. Larson, A. Poppe, D. Lawrence, R. Elphic, P. Hayne, et al., Nanoswarm: A cubesat discovery mission to study space weathering, lunar magnetism, lunar water, and small-scale magnetospheres, in: Lunar and Planetary Science Conference, 46, 2015, p. 3000.

[77] P. Clark, M. Collier, M. Schaible, W.M. Farrell, D. Folta, K.M. Hughes, J.W. Keller, B. Malphrus, A.S. Rivkin, S. Murchie, et al., Overview of phobos/deimos regolith ion sample mission (PRISM) concept, in: CubeSats and NanoSats for Remote Sensing II, Vol. 10769, International Society for Optics and Photonics, 2018, p. 107690I.

[78] N. Petro, E. Mazarico, X. Sun, J. Abshire, G. Neumann, P. Lucey, Miluv does it good—The mini lunar volatiles mission: A planetary science deep space smallsat study of a lunar orbiting mission, in: Lunar and Planetary Science Conference, Vol. 49, 2018.

[79] T. Hewagama, S. Aslam, P. Clark, M. Daly, L. Feaga, D. Folta, N. Gorius, T. Hurford, T. Livengood, B. Malphrus, M. Mumma, C. Nixon, J. Sunshine, G. Villanueva, A. Zucherman, Primitive object volatile explorer (PrOVE)-waypoints and opportunistic deep space missions to comets, 2018, http://dx.doi.org/10.1117/12.2321264.

[80] T. Stubbs, B. Malphrus, R. Hoyt, M. Mesarch, M. Tsay, D. Chai, M. Choi, M. Collier, J. Keller, W. Farrell, et al., Bi-sat observations of the lunar atmosphere above swirls (BOLAS): Tethered smallsat investigation of hydration and space weathering processes at the moon, in: Lunar and Planetary Science Conference, Vol. 49, 2018.

[81] R.W. Ebert, F. Allegrini, F. Bagenal, C.R. Beebe, M.A. Dayeh, M.I. Desai, D.E. George, J. Hanley, P. Mokashi, N. Murphy, et al., Jupiter magnetospheric boundary explorer (JUMPER), in: 2018 IEEE Aerospace Conference, IEEE, 2018, pp. 1–17.

[82] A. Didion, A. Komjathy, B. Sutin, B. Nakazono, A. Karp, M. Wallace, G. Lantoine, S. Krishnamoorthy, M. Rud, J. Cutts, et al., Remote sensing of venusian seismic activity with a small spacecraft, the VAMOS mission concept, in: 2018 IEEE Aerospace Conference, IEEE, 2018, pp. 1–14.

[83] NASA, What is capstone? 2020, URL https://www.nasa.gov/directorates/spacetech/small_spacecraft/capstone. (accessed Aug 2020).

[84] M.I. Desai, F. Allegrini, R.W. Ebert, K. Ogasawara, M.E. Epperly, D.E. George, E.R. Christian, S.G. Kanekal, N. Murphy, B. Randol, The CubeSat mission to study solar particles, IEEE Aerosp. Electron. Syst. Mag. 34 (4) (2019) 16–28, http://dx.doi.org/10.1109/maes.2019.2917802.

[85] NASA, Biosentinel fact sheet, 2019, URL https://www.nasa.gov/sites/default/files/atoms/files/biosentinel_fact_sheet-16apr2019_508.pdf. (accessed June 2020).

[86] J. Sobtzak, E. Tianang, B. Branham, N. Sonth, M. DeLuca, T. Moyer, S. Palo, A deep space radio communications link for CubeSats: The CU-E3 communication subsystem, 2017.

[87] S.H. Schaire, S. Altunc, Y.F. Wong, O.O. Kegege, G.D. Bussey, M. Murbach, H. Garon, Y. Dasgupta, S. Gaines, E. McCarty, et al., Investigation into new ground based communications service offerings in response to SmallSat trends, 2018.

[88] NASA, Cube quest challenge spotlight: Team miles, 2018, URL https://www.nasa.gov/directorates/spacetech/centennial_challenges/cubequest/team_miles. (accessed June 2020).

[89] C.J.G. David Folta, Navigation overview strategic and technical aspects of planetary small satellite missions, in: 3rd Planetary CubeSat Science Symposium Presentation Slides, 2018.

[90] S. Bhaskaran, Autonomous Navigation for Deep Space Missions, American Institute of Aeronautics and Astronautics, 2012, http://dx.doi.org/10.2514/6.2012-1267135.

[91] S. Bhaskaran, N. Mastrodemos, J.E. Riedel, S.P. Synnott, Optical navigation for the stardust wild 2 encounter, in: 18th International Symposium on Space Flight Dynamics, Vol. 548, 2004, p. 455.

[92] N. Mastrodemos, D.G. Kubitschek, S.P. Synnott, Autonomous navigation for the deep impact mission encounter with comet tempel 1, Space Sci. Rev. 117 (1–2) (2005) 95–121, http://dx.doi.org/10.1007/s11214-005-3394-4.

[93] A. Team, J. Riedel, S. Bhaskaran, S. Desai, D. Han, B. Kennedy, G. Null, S. Synnott, T. Wang, R. Werner, et al., Autonomous Optical Navigation (AutoNav) DS1 Technology Validation Report, Jet Propulsion Laboratory, California Institute of Technology, 2000.

[94] O. Camino, M. Alonso, D. Gestal, J. de Bruin, P. Rathsman, J. Kugelberg, P. Bodin, S. Ricken, R. Blake, P.P. Voss, et al., SMART-1 operations experience and lessons learnt, Acta Astronaut. 61 (1–6) (2007) 203–222.

[95] B. Segret, D. Hestroffer, G. Quinsac, M. Agnan, J. Vannitsen, On-board orbit determination for a deep space CubeSat, in: International Symposium on Space Flight Dynamics, 2017.

[96] T. Martin, A. Blazquez, E. Canalias, E. Jurado, J. Lauren-Varin, T. Ceolin, R. Garmier, J. Biele, L. Jorda, J.-B. Vincent, et al., Flight dynamics analysis for philae landing site selection, in: 25th International Symposium on Space Flight Dynamics, 2015.

[97] T. Oshima, J. Kawaguchi, S. Hagino, The mission operations of HAYABUSA asteroid explorer, in: 57th International Astronautical Congress, 2006, pp. C1–6.

[98] J.M. Rebordão, in: M.F.P.C.M. Costa (Ed.), Space Optical Navigation Techniques: an Overview, SPIE, 2013, http://dx.doi.org/10.1117/12.2026063.

[99] W.M. Owen Jr., Methods of Optical Navigation, Jet Propulsion Laboratory, National Aeronautics and Space ..., Pasadena, CA, 2011.

[100] C.J. Gramling, Planetary CubeSats deep space navigation, in: 4th Planetary CubeSat Science Symposium Presentation, 2019.

[101] B. Segret, J. Vannitsen, M. Agnan, A. Porquet, O. Sleimi, F. Deleflie, J.-J. Miau, J.-C. Juang, K. Wang, BIRDY: an interplanetary CubeSat to collect radiation data on the way to mars and back to prepare the future manned missions, in: Modeling, Systems Engineering, and Project Management for Astronomy VI, Vol. 9150, International Society for Optics and Photonics, 2014, p. 91501N.

[102] V.H. Adams, M.A. Peck, Interplanetary optical navigation, in: AIAA Guidance, Navigation, and Control Conference, American Institute of Aeronautics and Astronautics, 2016, http://dx.doi.org/10.2514/6.2016-2093.

[103] V.H. Adams, M.A. Peck, Lost in space and time, in: AIAA Guidance, Navigation, and Control Conference, American Institute of Aeronautics and Astronautics, 2017, http://dx.doi.org/10.2514/6.2017-1030.

[104] V. Franzese, F. Topputo, F. Ankersen, R. Walker, Deep-Space Optical Navigation for M-ARGO Mission, Springer Science and Business Media LLC, 2021, http://dx.doi.org/10.1007/s40295-021-00286-9.

[105] S.I. Sheikh, D.J. Pines, P.S. Ray, K.S. Wood, M.N. Lovellette, M.T. Wolff, American Institute of Aeronautics and Astronautics (AIAA), 2006, pp. 49–63, http://dx.doi.org/10.2514/1.13331.

[106] J. Getchius, A. Long, M. Farahmand, L.M. Winternitz, M.A. Hassouneh, J.W. Mitchell, Predicted performance of an X-Ray navigation system for future deep space and lunar missions, 2019.

[107] J.E. Hanson, Principles of X-ray Navigation, Tech. rep., Office of Scientific and Technical Information (OSTI), 2006, http://dx.doi.org/10.2172/877425.

[108] J. Dong, Pulsar navigation in the solar system, arXiv:0812.2635.

[109] K. Fujimoto, J. Leonard, R. McGranaghan, J. Parker, R. Anderson, G. Born, Simulating the Liaison Navigation Concept in a Geo+ Earth-Moon Halo Constellation, Pasadena, CA: Jet Propulsion Laboratory, National Aeronautics and Space ..., 2012.

[110] K. Hill, G.H. Born, Autonomous interplanetary orbit determination using satellite-to-satellite tracking, J. Guid. Control Dyn. 30 (3) (2007) 679–686, http://dx.doi.org/10.2514/1.24574.

[111] T. Qin, D. Qiao, M. Macdonald, Relative orbit determination using only intersatellite range measurements, J. Guid. Control Dyn. 42 (3) (2019) 703–710, http://dx.doi.org/10.2514/1.g003819.

[112] L. Markley, Autonomous Satellite Navigation Using Landmarks, Vol. -1, 1981.

[113] F. Markley, Autonomous navigation using landmark and intersatellite data, in: Astrodynamics Conference, 1987, p. 1987.

[114] J. Yim, J. Crassidis, J. Junkins, Autonomous orbit navigation of interplanetary spacecraft, in: Astrodynamics Specialist Conference, American Institute of Aeronautics and Astronautics, 2000, http://dx.doi.org/10.2514/6.2000-3936.

[115] A. Delépaut, P. Giordano, J. Ventura-Traveset, D. Blonski, M. Schönfeldt, P. Schoonejans, S. Aziz, R. Walker, Use of GNSS for lunar missions and plans for lunar in-orbit development, Adv. Space Res. 66 (12) (2020) 2739–2756.

[116] J.B. Berner, Deep space network in the CubeSat era, IEEE Aerosp. Electron. Syst. Mag. 34 (4) (2019) 46–54, http://dx.doi.org/10.1109/MAES.2019.2913266.

[117] M.L. Psiaki, Autonomous orbit determination for two spacecraft from relative position measurements, J. Guid. Control Dyn. 22 (2) (1999) 305–312, http://dx.doi.org/10.2514/2.4379.

[118] J.R. Yim, J.L. Crassidis, J.L. Junkins, 1 AAS 04-257 autonomous orbit navigation of two spacecraft system using relative line of sight vector measurements, 2004.

[119] Y. Gao, B. Xu, L. Zhang, Feasibility study of autonomous orbit determination using only the crosslink range measurement for a combined navigation constellation, Chin. J. Aeronaut. 27 (5) (2014) 1199–1210, http://dx.doi.org/10.1016/j.cja.2014.09.005.

[120] F. Meng, X. Wu, G. Ou, Autonomous orbit determination of navigation constellation based on inter-satellite ranging and ranging rate, J. Spacecr. TT C Technol. 29 (4) (2010) 89–94.

[121] S. Hesar, J. Parker, J. Mcmahon, G. Born, Small body gravity field estimation using LiAISON supplemented optical navigation, 2015.

[122] J. Leonard, B. Jones, E. Villalba, G. Born, Absolute orbit determination and gravity field recovery for 433 eros using satellite-to-satellite tracking, in: AIAA/AAS Astrodynamics Specialist Conference, American Institute of Aeronautics and Astronautics, 2012, http://dx.doi.org/10.2514/6.2012-4877.

[123] W. Wang, L. Shu, J. Liu, Y. Gao, Joint navigation performance of distant retrograde orbits and cislunar orbits via LiAISON considering dynamic and clock model errors, Navigation 66 (4) (2019) 781–802, http://dx.doi.org/10.1002/navi.340.

[124] N. Stacey, S. D'Amico, (Preprint) AAS 18-448 autonomous swarming for simultaneous navigation and asteroid characterization, 2018.

[125] K. Hill, J. Parker, G. Born, N. Demandante, A lunar L2 navigation, communication, and gravity mission, in: AIAA/AAS Astrodynamics Specialist Conference and Exhibit, American Institute of Aeronautics and Astronautics, 2006, http://dx.doi.org/10.2514/6.2006-6662.

[126] K.A. Hill, G.H. Born, Autonomous orbit determination from lunar halo orbits using crosslink range, J. Spacecr. Rockets 45 (3) (2008) 548–553, http://dx.doi.org/10.2514/1.32316.

[127] J.M. Leonard, Supporting Crewed Missions using LiAISON Navigation in the Earth-Moon System (Ph.D. thesis), University of Colorado, 2015.

[128] K. Fujimoto, N. Stacey, J.M. Turner, Stereoscopic image velocimetry as a measurement type for autonomous asteroid gravimetry, in: AIAA/AAS Astrodynamics Specialist Conference, American Institute of Aeronautics and Astronautics, 2016, http://dx.doi.org/10.2514/6.2016-5566.

[129] C. Duncan, Low mass radio science transponder – navigation anywhere, 2012, URL https://icubesat.org/papers/2012us/2012-c-3-2/.

[130] M. D., Autonomous Relative Navigation for Small Spacecraft (Ph.D. thesis), Delft University of Tecnology, 2014.

[131] S. Bertone, C. Le Poncin-Lafitte, P. Rosenblatt, V. Lainey, J.-C. Marty, M.-C. Angonin, Impact analysis of the transponder time delay on radio-tracking observables, Adv. Space Res. 61 (1) (2018) 89–96.

[132] E.C. for Space Standardization, ECSS-E-ST-50-02C - Ranging and Doppler tracking, Tech. rep., 2018.

[133] H.W. Baugh, Sequential Ranging: How It Works, Vol. 94, NASA STI/Recon Technical Report N, 1993, p. 13796.

[134] S.E.S. European Telecommunications Standards Institute, S. (SES), Satellite Earth Stations and Systems (SES);Technical analysis of Spread Spectrum Solutionsfor Telemetry Command and Ranging (TCR)of Geostationary Communications Satellites, Tech. rep., 2001, URL https://www.etsi.org/deliver/etsi_tr/101900_101999/101956/01.01.01_60/tr_101956v010101p.pdf.

[135] M.B. Mwakyanjala, M.R. Emami, J. van de Beek, Functional analysis of software-defined radio baseband for satellite ground operations, J. Spacecr. Rockets 56 (2) (2019) 458–475, http://dx.doi.org/10.2514/1.a34333.

[136] DSN Telecommunications Link Design Handbook, Tech. rep., Jet Propulsion Laboratory California Institute of Technology, 2018, URL http://deepspace.jpl.nasa.gov/dsndocs/810-005/.

[137] J.L. Massey, G. Boscagli, E. Vassallo, Regenerative pseudo-noise (PN) ranging sequences for deep-space missions, Int. J. Satell. Commun. Netw. 25 (3) (2007) 285–304, http://dx.doi.org/10.1002/sat.877.

[138] J.B. Berner, S.H. Bryant, P.W. Kinman, Range measurement as practiced in the deep space network, Proc. IEEE 95 (11) (2007) 2202–2214, http://dx.doi.org/10.1109/jproc.2007.905128.

[139] CCSDS, Proximity-1 Space Link Protocol - Physical Layer CCSDS 211.1-B-4, Tech. rep., 2013, URL https://public.ccsds.org/Pubs/211x1b4e1.pdf.

[140] C.T.C.C. for Space Data Systems, Proximity-1 Space Link Protocol - Data Link Layer Recommended Standard, Tech. rep., 2020, July 2020.

[141] S. Woo, J. Gao, D. Mills, Space network time distribution and synchronization protocol development for mars proximity link, in: SpaceOps 2010 Conference, American Institute of Aeronautics and Astronautics, 2010, http://dx.doi.org/10.2514/6.2010-2360.

[142] Time synchronization for space data links, 2012, URL http://www.cis.udel.edu/~mills/proximity.html.

[143] G. Iraci, C. Gnam, An open source radio for low cost small satellite ranging, 2018.

[144] C. Foster, H. Hallam, J. Mason, Orbit determination and differential-drag control of planet labs cubesat constellations, arXiv:http://arxiv.org/abs/1509.03270v1.

[145] J. Hamkins, P. Kinman, H. Xie, V. Vilnrotter, S. Dolinar, Telemetry ranging: Concepts, in: IPNPR, Vol. 42, 2015, pp. 1–20.

[146] K. Andrews, J. Hamkins, S. Shambayati, V. Vilnrotter, Telemetry-based ranging, in: 2010 IEEE Aerospace Conference, IEEE, 2010, pp. 1–16.

[147] C.T.C.C. for Space Data Systems, Pseudo-Noise (PN) Ranging Systems, Tech. rep., 2014, February 2014.

[148] S. Bryant, J. Berner, Operations comparison of deep space ranging types: sequential tone vs. pseudo-noise, 2002.

[149] S.W. Asmar, J.W. Armstrong, L. Iess, P. Tortora, Spacecraft Doppler tracking: Noise budget and accuracy achievable in precision radio science observations, Radio Sci. 40 (2) (2005) http://dx.doi.org/10.1029/2004rs003101.

[150] R. Sun, D. Maessen, J. Guo, E. Gill, Enabling inter-satellite communication and ranging for small satellites, in: 9th Symposium on Small Satellites Systems and Services, Funchal, Portugal, 31, 2010.

[151] L. Iess, M.D. Benedetto, N. James, M. Mercolino, L. Simone, P. Tortora, Astra: interdisciplinary study on enhancement of the end-to-end accuracy for spacecraft tracking techniques, Acta Astronaut. 94 (2014) 699–707, http://dx.doi.org/10.1016/j.actaastro.2013.06.011.

[152] C.L. Thornton, J.S. Border, Radiometric Tracking Techniques for Deep Space Navigation, John Wiley & Sons, Inc. 2003, http://dx.doi.org/10.1002/0471728454.

[153] M. Zannoni, P. Tortora, Numerical error in interplanetary orbit determination software, J. Guid. Control Dyn. 36 (4) (2013) 1008–1018, http://dx.doi.org/10.2514/1.59294.

[154] A. Tiainen, Inter-satellite link antennas: Review and the near future, 2017.

[155] R. Funase, H. Koizumi, S. Nakasuka, Y. Kawakatsu, Y. Fukushima, A. Tomiki, Y. Kobayashi, J. Nakatsuka, M. Mita, D. Kobayashi, et al., 50Kg-class deep space exploration technology demonstration micro-spacecraft PROCYON, 2014.

[156] M.M. Kobayashi, S. Holmes, A. Yarlagadda, F. Aguirre, M. Chase, K. Angkasa, B. Burgett, L. McNally, T. Dobreva, E. Satorius, The iris deep-space transponder for the SLS EM-1 secondary payloads, IEEE Aerosp. Electron. Syst. Mag. 34 (9) (2019) 34–44, http://dx.doi.org/10.1109/maes.2019.2905923.

[157] M. Kobayashi, Iris deep-space transponder for SLS EM-1 CubeSat missions, 2017.

[158] J.P. Laboratory, Iris V2 CubeSat deep-space transponder (IRIS), 2019, URL https://www.jpl.nasa.gov/cubesat/missions/iris.php.

[159] T. Hashimoto, T. Yamada, M. Otsuki, T. Yoshimitsu, A. Tomiki, W. Torii, H. Toyota, J. Kikuchi, N. Morishita, Y. Kobayashi, T. Ito, H. Tanno, A. Nagamatsu, H. Morimoto, Nano semihard moon lander: OMOTENASHI, IEEE Aerosp. Electron. Syst. Mag. 34 (9) (2019) 20–30, http://dx.doi.org/10.1109/maes.2019.2923311.

[160] S. Palo, D. O'Connor, E. DeVito, R. Kohnert, G. Crum, S. Altunc, Expanding CubeSat capabilities with a low cost transceiver, 2014.

[161] J. Schoolcraft, A. Klesh, T. Werne, MarCO: interplanetary mission development on a CubeSat scale, in: Space Operations: Contributions from the Global Community, Springer, 2017, pp. 221–231.

[162] M.R. Maheshwarappa, C.P. Bridges, Software defined radios for small satellites, in: 2014 NASA/ESA Conference on Adaptive Hardware and Systems, AHS, IEEE, 2014, pp. 172–179.

[163] C. Loisel, C. Dudal, O. Bompis, H. Guillon, F. Rousseau, G. Liabeuf, J. Issler, InterSatellite Links for Rosetta/Philae, Hayabusa-2/Mascot, and next-gen miniaturized ISL in S and Ka band.

[164] G. Dynamics, Small Deep Space Transponder, http://gdmissionsystems.com (Accessed 04 December 2020).

[165] M.B. O'Neill, C.B. Haskins, B.M. Bubnash, Advances in deep space radios, in: 2017 IEEE MTT-S International Microwave Symposium, IMS, IEEE, 2017, pp. 398–401.

[166] M. Pugh, I. Kuperman, F. Aguirre, H. Mojaradi, C. Spurgers, M. Kobayashi, E. Satorius, T. Jedrey, The universal space transponder: A next generation software defined radio, in: 2017 IEEE Aerospace Conference, IEEE, 2017, pp. 1–14.

[167] M.M. Kobayashi, State-Of-The-Art Status for Deep-Space Smallsat Telecom, Pasadena, CA: Jet Propulsion Laboratory, National Aeronautics and Space ..., 2018.